

Investigation of possible non-additive behavior in the formation  
of secondary organic aerosol from a mixture of anthropogenic  
and biogenic VOC precursors

John Falk

Master's Thesis  
Engineering Physics

---

Division of Nuclear Physics  
Department of Physics  
Lund University

June 11, 2014

Contact: [jaget@johnfalk.se](mailto:jaget@johnfalk.se)  
Supervisors:  
Erik Swietlicki  
Birgitta Svenningsson

### Abstract

Secondary organic aerosol (SOA) mass yields were tested for six combinations of two anthropogenic volatile organic compounds (AVOC); m-xylene & toluene, and three biogenic volatile organic compounds (BVOC);  $\alpha$ -pinene, myrcene & isoprene. The purpose was to investigate any non-additive results in SOA formation from mixtures of AVOCs and BVOCs by comparing experimental yield with corresponding two-product model yields. No seed particles were used. Mass and number size distributions from generated SOA was investigated. The measurements were performed by aging the VOC gases using a potential aerosol mass (PAM) chamber and measuring the resulting SOA mass with a scanning mobility particle sizer (SMPS), and to a limited extent an aerosol mass spectrometer (AMS). AMS data was used to calculate an average SOA density of  $\approx 2.0 \text{ g cm}^{-3}$ , although for calculations a value  $\approx 1.4 \text{ g cm}^{-3}$  was used. The VOC air flow was at  $RH = 30.6 \pm 0.3\%$ , and PAM chamber  $\text{O}_3$  concentrations were for all experiments  $5400 \pm 880$  ppb. Differences in experimental and model yields were observed with a maximum difference of 30 % and a minimum of 4 %, although for all experiments model yields were mostly or completely inside experimental uncertainty limits, and so no non-additive effects could be concluded. Aging of a mixture with isoprene added showed a factor  $\approx 4$  decrease in overall number concentration, and a slight shift of mass size distribution to larger particle sizes. The experiment set-up used was also investigated, and showed several shortcomings. Most notably was the uncertainty regarding VOC emission rate, to a part caused by a lack of instrumentation measuring diffusion chamber parameters.



# Contents

<b>List of abbreviations</b>	<b>vi</b>
<b>1 Introduction</b>	<b>1</b>
1.1 Background . . . . .	1
1.2 Aim . . . . .	1
<b>2 Theory</b>	<b>2</b>
2.1 SOA formation chemistry . . . . .	2
2.2 Particle equivalent diameter . . . . .	2
2.3 Theoretical emission rates . . . . .	3
2.4 SOA Yield . . . . .	3
2.4.1 Experimental yield . . . . .	3
2.4.2 Two-product model yield . . . . .	3
<b>3 Methodology</b>	<b>4</b>
3.1 Summary . . . . .	4
3.2 PTR-MS trials . . . . .	4
3.3 Experiment set-up . . . . .	4
3.4 PAM chamber . . . . .	5
3.5 Diffusion chamber . . . . .	7
3.6 Air humidity control system . . . . .	7
3.7 VOCs . . . . .	7
3.8 VOC emission rates . . . . .	8
3.9 SMPS . . . . .	8
3.10 AMS . . . . .	10
3.11 Measurements . . . . .	10
3.12 Data analysis . . . . .	11
3.12.1 SOA yields . . . . .	11
3.12.2 Two-product model comparison . . . . .	12
3.13 Uncertainty limits . . . . .	12
<b>4 Results &amp; discussion</b>	<b>13</b>
4.1 SOA yields . . . . .	13
4.1.1 $\alpha$ -pinene & m-xylene . . . . .	15
4.1.2 m-xylene & isoprene . . . . .	17
4.1.3 Myrcene & m-xylene . . . . .	17
4.1.4 Myrcene, m-xylene & $\alpha$ -pinene . . . . .	19
4.1.5 Myrcene, m-xylene, $\alpha$ -pinene & isoprene . . . . .	20
4.1.6 Toluene & $\alpha$ -pinene . . . . .	21
4.2 Number concentrations in relation to isoprene . . . . .	22
<b>5 Set-up evaluation</b>	<b>23</b>
<b>6 Conclusion</b>	<b>24</b>
<b>Acknowledgments</b>	<b>25</b>
<b>References</b>	<b>26</b>
<b>Appendix A: MATLAB code</b>	<b>29</b>
<b>Appendix B: Experiment data</b>	<b>34</b>

## List of abbreviations

AMS - Aerosol Mass Spectrometer

AVOC - Anthropogenic Volatile Organic Compound

BVOC - Biogenic Volatile Organic Compound

CPC - Condensation Particle Counter

DMA - Differential Mobility Analyzer

HC - Hydrocarbon

MFC - Mass Flow Controller

OH - hydroxyl

PAM - Potential Aerosol Mass

RH - Relative Humidity

PTR-MS - Proton Transfer-Rate Mass Spectrometer

SMPS - Scanning Mobility Particle Sizer

SOA - Secondary Organic Aerosol

VOC - Volatile Organic Compound

# 1 Introduction

## 1.1 Background

Aerosols are defined as solid or liquid particles suspended in a gas such as air. Secondary organic aerosol (SOA) is a subgroup of these, which are produced naturally in the atmosphere by means of oxidation of volatile organic compounds (VOC). SOA can make up a range of properties in the atmosphere, such as scatter light, absorb light, but also act as cloud condensation nuclei in forming clouds. Although exact definitions vary, VOCs are a group of organic chemicals which generally have a low boiling point at atmospheric conditions, causing them to evaporate.

Atmospheric secondary organic aerosols (SOA) have become an increasingly researched subject in recent years. This is originating from the fact that still very little is understood about the processes surrounding them, and that these particles can have potentially significant implications on both the Earth's climate and human health.

There is a very large uncertainty as to the global atmospheric SOA production levels. Current estimates range from 50 - 380 Tg yr<sup>-1</sup> (Spracklen et al., 2011), although older studies suggest estimates ranging from 12 - 1820 Tg yr<sup>-1</sup> (Kanakidou et al., 2005; Goldstein and Galbally, 2007; Hallquist et al., 2009; Spracklen et al., 2011)<sup>1</sup>. This leads to large uncertainties in other areas, not least how SOA contributes to the Earth's radiative forcing. Currently, atmospheric SOAs effect on the radiative forcing is estimated to be somewhere between -0.4 and +0.1 W m<sup>-2</sup> (Boucher and Zhang, 2013).

In addition to this, particulate matter such as SOA is also associated with a range of negative health effects mainly related to the pulmonary or cardiovascular systems (Davidson et al., 2005; Pope and Dockery, 2006). It would therefore be of importance to learn sufficiently about these compounds in order to be able to mitigate any future complications they may lead to.

VOCs can be divided into two subgroups. Biogenic (BVOC); VOCs produced and emitted by natural processes mainly in plants, and

Anthropogenic (AVOC); VOCs produced and emitted by means of human activity such as petroleum combustion. Although large uncertainties persist also on the specific global emissions of VOCs, most research indicate that BVOCs stands for a large majority of produced atmospheric SOA (Spracklen et al., 2011; Kanakidou et al., 2005; Heald et al., 2011; Goldstein and Galbally, 2007). As this may be, locally such as in urban areas, AVOCs may take a majority role in SOA production (Fushimi et al., 2011).

It has previously been suggested that atmospheric aging of a mixture between AVOCs and BVOCs would lead to an enhanced amount of SOA formation. (Volkamer et al., 2006; Hoyle et al., 2011; Heald et al., 2011), This more specifically meaning that had the AVOC and BVOC components been aged separately, at the same conditions as the mixture, then their combined amount of formed SOA would have been lower from that of the mixture. This was recently reported by Setyan et al. (2012). The study observed outside organic aerosol to carbon monoxide ratios ( $\Delta\text{OA}/\Delta\text{CO}$ ) to look at indications of SOA production levels, and found that this ratio was largest when the studied air mass contained high levels of both AVOCs and BVOCs. Shen et al. (2013) have more generally laid forward that heterogeneous VOC combinations might prove to affect SOA formation.

(Emanuelsson et al., 2013) on the other hand, while noticing an overall difference in volatility in produced SOA from AVOC and BVOC mixtures, found no such relation in SOA production.

## 1.2 Aim

This thesis aim is to investigate these theories of non-additivity for some selected combinations of VOCs. It will be guided by exploring the following research questions:

- Are there any non-additive effects relating to SOA formation for selected AVOC and BVOC mixtures compared to individual VOCs?

<sup>1</sup>Upper estimate calculated by Spracklen et al. (2011) based on data from given sources.

- How is particle size distribution and number concentration affected by mixing the selected VOCs?
- What are the advantages/disadvantages of the experimental set-up that was used?

Chapter 1 presents the background motivation and aim for this thesis. Chapter 2 describes relevant theory connected to the experiments and analysis of data. It presents more in detail the chemistry behind SOA formation related to these experiments. It also explains the particle detection method which was used, and present the mathematical theory of which the data analysis is based on.

Chapter 3 explains the experiment set-up and how experiments as well as analysis were performed. Here it discusses the layout of the experiment set-up and its components, as well as the function of these components. It explains in detail procedures used for handling the VOCs, how the measurements were performed, and how the data analysis was performed. Uncertainty limits are stipulated in section 3.13.

Chapter 4 presents the results and a discussion surrounding them. For each studied mixture SOA yields as well as number and mass size distributions are presented and discussed. Comparisons between the individual VOCs experimental and model yield are presented here as well.

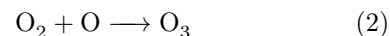
Chapter 5 will discuss and evaluate the experimental set-up itself, and present shortcomings and possible improvements to be made. Chapter 6 summarizes the main conclusions from this work and present an outlook for future work.

## 2 Theory

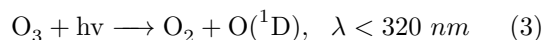
### 2.1 SOA formation chemistry

SOA is formed in the atmosphere from oxidation of organic compounds such as VOCs, causing them to grow. This process involves interaction with hydroxyl (OH) radicals, and is often referred to as atmospheric aging of the compound. A Potential Aerosol Mass (PAM) reactor chamber (Kang et al., 2007) can simulate this process at 100 to 10,000 times higher concentrations of OH radicals, which causes aging to happen at a faster

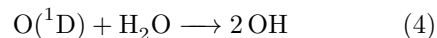
rate. This makes PAM measurements more time-efficient than natural atmospheric aging. Initially  $O_3$  is formed in the PAM through UV radiation which interacts with oxygen gas according to the reactions



Excited  $O(^1D)$ -atoms are created through photolysis ( $\lambda = 254 \text{ nm}$ ) of  $O_3$



These excited oxygen atoms in turn reacts with water vapor from incoming flow (in these experiments  $RH = 30.6 \pm 0.3 \%$ ) to create OH radicals through



which are then reacting with the introduced compounds.

### 2.2 Particle equivalent diameter

For the most part when studying aerosols, what you have is a collection of irregularly shaped particles. This is often true even when looking at more specific types of aerosols; soot being a good example. Soot particles are a chaotic conglomerate of smaller particles, sometimes with an almost tree-like structure. Because of this depending on what property one desire to study, basic physical form for example could be very mis-representative to density. However, there are cases where the shape is the property of interest; such as with nano-tubes and their ability to penetrate living tissue and so on.

Instead, something called equivalent diameter is often used in aerosol measurement techniques. This concept instead categorizes the studied aerosols and assigns a diameter by how they act in certain settings compared to a perfectly spherical particle. This can be aerodynamically, optically, electromagnetically and so on.

In this thesis, a Scanning mobility particle sizer was used. This device measures the so-called *electric mobility equivalent diameter* of a particle, which looks at how movement of charged particles are influenced by an electromagnetic field. The



particles are charged with a radioactive source prior to entering the device. Based on how much the charged particles are then influenced to drift perpendicular to the main air or liquid flow direction, an equivalent diameter is calculated. This is derived from what diameter a spherical particle with the same charge would have in order to be equally affected by the electromagnetic field. This is done through the equation

$$Z_p = \frac{neC_c}{3\pi\eta D_p} \quad (5)$$

where  $Z_p$  is electric mobility ( $m^2 V s^{-1}$ );  $n$  the particles' number of charges;  $e$  elemental charge;  $C_c$  Cunningham slip correction factor, which is dependent on particle diameter;  $\eta$  absolute viscosity of air ( $kg/ms^{-1}$ ); and  $D_p$  diameter of the particle ( $m$ ). The equation is derived from Stokes' Law.

### 2.3 Theoretical emission rates

Theoretical emission rates for a compound in a volume with an attached capillary can be obtained by applying (McKelvey and Hoelscher, 1957)

$$r = \frac{DMAP_0}{RTL} \ln\left(\frac{P_0 - P}{P}\right) \quad (6)$$

where  $r$  is emission rate ( $g s^{-1}$ );  $D$  diffusion constant ( $m^2 s^{-1}$ ) at pressure  $P_0$ ,  $P_0$  being 105.8  $kPa$  in these experiments;  $M$  compound molar weight ( $g mol^{-1}$ );  $A$  capillary cross-sectional area ( $m^2$ );  $R$  the gas constant ( $m^3 Pa mol^{-1} K^{-1}$ );  $T$  absolute temperature ( $K$ );  $L$  length of capillary ( $m$ );  $P_0$  total pressure acting on the system ( $Pa$ ), and  $P$  specific vapor pressure ( $Pa$ ).

Diffusion constant  $D$  for each VOC in the experiments was estimated based on a mean of three different methods for calculating diffusion constants: The FSG method, which is based on a regression formula taking into account temperature, pressure, molar weights and molar volumes (Fuller et al., 1966); the FSG-LeBas method, which is a modified version of the FSG method that instead uses LeBas molar volume estimates in place of molar volumes (Lyman, 1990); the WL method, which is based on a series of calculations of a collision integral representing collisions between atoms, also taking into account temperature, pressure and LeBas molar volume estimates (Wilke and Lee, 1955).

Equation (6) assumes that the gas-phase of the compound in the vial is saturated, and that the concentration of the compound vapor in the outside medium is approximately zero.

Vapor pressure for the compound can be estimated with the Antoine equation (Thomson, 1946)

$$\log_{10}(P) = A - \frac{B}{C + T} \quad (7)$$

where  $A, B$  and  $C$  are compound specific constants and  $T$  is absolute temperature ( $K$ ).

## 2.4 SOA Yield

### 2.4.1 Experimental yield

The SOA yield  $Y$  is defined as the generated SOA mass concentration from the reacted precursor VOC mass concentration, or

$$Y = \frac{M_0}{\Delta HC} \quad (8)$$

where  $Y$  is yield;  $M_0$  SOA mass concentration;  $\Delta HC$  VOC mass concentration. (Pankow, 1994b,a; Odum et al., 1996)

A true chemist would point out that this is not really a yield since, from a chemical standpoint, the VOC mass is actually reacting with OH to form the SOA, and the reacting OH mass is not considered in this equation. In spite of this, it is a well established term and will be referred to as a yield here.

$M_0$  in these experiments was derived from volume concentration according to

$$M_0 = V_{conc,soa} * \rho_{soa} \quad (9)$$

$V_{conc,soa}$  being the SOA volume concentration ( $\mu m^3 cm^{-3}$ ) and  $\rho_{SOA}$  the average SOA density ( $g cm^{-3}$ ).

### 2.4.2 Two-product model yield

The two-product model can be used to approximate a compounds SOA yield for a given SOA mass concentration. Based on these models it is also possible to construct an additive approximation for the yield for a mixture of compounds.

The model is defined as (Pankow, 1994*b,a*; Odum et al., 1996)

$$Y_{2p}(M_0) = M_0 \left( \frac{\alpha_1 * k_{om,1}}{1 + k_{om,1} * M_0} + \frac{\alpha_2 * k_{om,2}}{1 + k_{om,2} * M_0} \right). \quad (10)$$

where  $M_0$  is measured SOA mass concentration;  $Y_{2p}(M_0)$  the model yield as a function of SOA mass concentration;  $\alpha_{1,2}$  mass-based gas-phase stoichiometric factors;  $k_{om,1,2}$  gas-phase partitioning coefficients.  $2p$  denotes two-product model derived values.

By using the two-product model of corresponding VOC in a mixture, it is possible to calculate that VOCs theoretical SOA mass concentration at the related measured mixture SOA mass concentration

$$M_{2p,VOC1}(M_0) = Y_{2p,VOC1}(M_0) * \Delta HC_{M_0,VOC1} \quad (11)$$

where  $M_{2p,VOC1}(M_0)$  is theoretical SOA mass concentration for a compound  $VOC1$  at measured mixture SOA mass concentration  $M_0$ ;  $Y_{2p,VOC1}(M_0)$  the theoretical yield;  $\Delta HC_{M_0,VOC1}$  experimental VOC mass concentration.

From this, the mixtures total theoretical SOA mass concentration is given by adding all individual VOCs contributions

$$M_{2p,mixture} = M_{2p,VOC1} + M_{2p,VOC2} + \dots + M_{2p,VOCN}. \quad (12)$$

and from that the theoretical SOA yield

$$Y_{2p,mixture} = \frac{M_{2p,mixture}}{\Delta HC}. \quad (13)$$

## 3 Methodology

### 3.1 Summary

The experiments were centered around use of the Potential Aerosol Mass (PAM) chamber. This device would provide simulation of atmospheric aging processes via oxidization of precursory gases. The simulated aging would correspond to 5-6 days of atmospheric aging ( $OH_{exp} \approx 7 * 10^{11} \text{ cm}^{-3} \text{ s}$ ).

The thesis would study the resulting SOA yield from mixtures of AVOCs; m-xylene, toluene,

and BVOCs;  $\alpha$ -pinene, myrcene and isoprene, and compare experimental yield with an additive model yield. First each individual VOC was aged separately in order to calculate a corresponding additive model based on the two-product model (section 2.4.2) for each mixture. Following this, each VOC mixture was aged, and the resulting SOA yield was compared to corresponding two-product model.

In addition to SOA yield, SOA size distributions were also studied and compared to that of the individual VOCs. An Aerodyne Aerosol Mass Spectrometer (AMS) was connected to the set-up and used to estimate the density of produced SOA.

The experiment set-up was based on having purified dry air running through a sealed chamber containing VOC vials with capillaries attached (Figure 1). The resulting VOC populated flow ( $Q_1$ ) would be adjusted by diverting part of it to a sink ( $Q_3$ ). The flow would continue be mixed with a humid air flow ( $Q_2$ ), and continue into the PAM chamber ( $Q_{7a}$ ) for aging. An Aerosol Mass Spectrometer (AMS) and a Scanning Mobility Particle Sizer (SMPS) were used to collect data on the produced aerosols.

### 3.2 PTR-MS trials

The VOC vials and capillaries were measured with a proton transfer-rate mass spectrometer (PTR-MS) prior to starting the main experiment campaign. This was performed to evaluate several set-up parameters such as suitable capillaries for each VOC; water bath temperature; VOC emission rate and stability; and to investigate how well the custom-built diffusion system worked overall.

### 3.3 Experiment set-up

The experiment set-up can be viewed in Figure 1, where relevant flows are denoted  $Q_{\#}$ . The set-up was based mainly on 1/4 inch steel piping with *Swagelok* connections. A diffusion chamber for the studied VOCs was connected upstream from the PAM chamber, and the diffusion chamber was set to have a constant flow,  $Q_1$  in Figure 1, of purified dry air running through it throughout the experiments. The diffusion chamber as well as some length of steel piping pre-diffusion

chamber was partially submerged in a water bath (GRANT SUB Aqua Pro) with distilled water of a constant temperature 24 °C, to allow an as stable evaporation of the VOCs as possible. The purified air was supplied from compressed air running through a zero air generator (LNI Schmidlin GT-30000), and the flow  $Q_1$  was set with a needle valve.

All controlled flows in the experiment set-up were regulated either with needle valves, or computer controlled mass flow controllers. The exception being a gate valve on the  $Q_4$  line.  $Q_4$  was the flow that was regulated to attain different mass concentrations for the VOCs coming from the diffusion chamber. The gate valve had the purpose of sealing the main line in order to reroute the flow through a flow meter (TSI 4100 Series), when such a device was connected in parallel over the gate valve. The  $Q_1$  flow wasn't regularly checked for fluctuations, although the largest fluctuation observed was 0.08  $l/min$  during a 4 hour interval, 6 - 8 hours being a typical complete session. Between experiment days  $Q_1$  varied significantly more, and the flow was observed to change as much 0.2  $l/min$ . This was assumed to be at least partially due to the varying atmospheric pressure, which varied between 99.37 - 102.9  $kPa$ .

The relative humidity of the flow entering the PAM chamber was  $30.6 \pm 0.3$  % and was controlled via a separate humid air flow,  $Q_2$ , of a constant flow 6.0  $l/min$  whose humidity was regulated by mass flow controllers and a humidifier. The  $Q_2$  flow merged with the main flow post-diffusion chamber, pre-PAM chamber. No mixing volume was utilized prior to the flow entering the PAM chamber, as it was deemed unnecessary. A connection port for extra VOC flows  $Q_{iso}$ , specifically used including isoprene which was supplied by gas tank, was located just before the  $Q_6$  flow.

A charcoal denuder was connected directly after the PAM chamber to try to reduce  $O_3$  and minimize the risk of damaging the detection instrumentation. The set-up was tested without a denuder to check if it interfered with the measurements, and showed no noticeable change

in measured aerosol mass. The PAM chamber was subject to a flow  $Q_{10}$  caused by suction downstream which was regulated by a needle valve. This flow was set so that the flow  $Q_{7a}$ , into the PAM chamber was always 5  $l/min$ . This meant an average particle residence time of  $\tau = 162$  s. The AMS and SMPS were connected to the  $Q_{10}$  flow, and since these devices required flows of 0.2  $l/min$  and 1  $l/min$  respectively,  $Q_{10}$  had to be smaller than  $Q_{7a}$ . The difference between flows  $Q_6$  and  $Q_{7a}$ ,  $Q_6$  always being larger than  $Q_{7a}$ , was handled by the excess flow drain,  $Q_5$ . This flow was exposed to atmospheric pressures downstream so as to affect the upstream flows to a minimal extent. An  $O_3$  monitor (Thermo Scientific 49i) was connected through a separate outlet on the downstream end of the PAM chamber.

### 3.4 PAM chamber

The PAM chamber is a tool for generating secondary organic aerosols (SOA) by creating a highly-oxidizing environment with a continuous flow of reacting material, in a relatively small volume by means of a controlled UV radiation source. (Kang et al., 2007; Lambe et al., 2011). It is used for simulating atmospheric oxidation processes, and is a complement to other methods such as chambers where batches of reacting material are instead studied. One such example is the SAPHIR chamber in Jülich, Germany (Dorn et al., 2013).

The shorter time intervals involved per measurement, requiring on an order of minutes rather than hours or days for other methods as well as working with continuous flows rather than batch-wise measurements can be very advantageous, especially when looking at scenarios with individual variable changes. In addition to this, the PAM concept allows for a larger environmental control since the radiation itself is controlled.

The PAM chamber is not without faults, as not only do the higher concentrations of oxidizing particles involved potentially skew results when comparing to atmospheric processes, but neither does the PAM UV emission spectrum fully represent the atmospheric counterpart, which might further affect representation. The chamber



### 3.5 Diffusion chamber

The VOCs entering the PAM were introduced to the air flow by means of diffusion inside a modified glass container; in this thesis referred to as a diffusion chamber. This chamber was made from a glass container, and a plastic lid with an inner coating of Teflon to minimize contamination and uptake of the hosted compounds. Since the container was made out of glass and would be exposed to pressure, its outside was lined with tape to contain any eventual shattering. The container was never exposed to any large pressures, typically 103–108  $kPa$ , but as the set-up didn't contain any specific relief valves a stoppage could potentially have lead to a pressure build-up in the chamber. The plastic lid had three flow ports; one center port for incoming flow, with Teflon piping to reach near the bottom of the container; one port for outgoing flow and one closed port for measuring pressure. A custom metal cylinder was located at the bottom of the container, with four circular depressions where the VOC vials were to be placed. A hole ran through the center of the cylinder, and its underneath was grooved to allow the plastic piping from the center flow port to direct the incoming air around the rim of the cylinder and upwards, past the VOC vials. The cylinder also had a number of vertical holes through it to allow air flowing upwards also there, and help in trying to create an as laminar air flow around the vials as possible.

### 3.6 Air humidity control system

This system was supplied with purified dry air from the same zero air flow as the main flow  $Q_1$ . It consisted of a flow  $Q_2$  regulated by a mass flow controller, denoted *Mass flow controller 1* in Figure 1, which was set to always have a flow of 6  $l/min$ . This flow was then divided into two separate flows,  $Q_{2a}$  and  $Q_{2b}$ . The primary line was  $Q_{2a}$ , which had another mass flow controller, *Mass flow controller 2*, followed by an air humidifier. The humidifier was a water-filled cylinder with tubing made of Gore-Tex submerged in it, allowing small amounts of water to penetrate the Gore-Tex material and enter the air stream. Ultra pure water was used in the humidifier. The purpose of  $Q_{2b}$  was to redirect the remaining flow which did not flow through  $Q_{2a}$ , creating a con-

stant flow while adapting humidity. An RH monitor was located in an excess flow drain  $Q_5$  prior to the PAM chamber. Both the RH monitor and the mass flow controllers were connected to a computer via a DAQ card and controlled via National Instruments *LabView 7.0*, which was configured to work as a PID-regulator for the humidity level. The PID settings were;  $P = 0.1$ ;  $I = 0.02$ ;  $D = 0.002$ . It is unclear if there was any significant advantage to include such a small D-term but as the configuration proved to function well, it was not further looked into.

### 3.7 VOCs

All VOCs studied with the exception of isoprene were handled in liquid form. Because of this, introduction of isoprene to the experiment VOC flow had to be handled differently and independent from the diffusion chamber system. Isoprene was supplied from a gas tank through a connection port  $Q_{iso}$  seen in Figure 1, and was held at a constant flow of 0.5  $l/min$  throughout most experiments. The reasoning behind this was that by keeping the isoprene flow constant and the same for all experiments containing isoprene, it would be easier to compare results. The VOCs used are listed in Table 1.

The liquid form VOCs were put in glass vials, typically in quantities of 0.3 to 1.0  $mL$ . The exact volumes for each individual compound weren't deemed relevant for the experiments, as long as the compounds filled up a noticeable portion of the vial and were used together with capillaries. A gas-tight syringe was used to transfer the compounds, and great care was taken not to contaminate the compounds. The syringe was rinsed with ethanol, acetone and distilled water before and after each use. In some cases there was unavoidable residue coming from the original vials septum, which had to be penetrated and left small plastic bits. This was assumed not to interfere with diffusion of the compound, and thus not an issue. The vials were stored sealed in a plastic bag in a fume collecting environment between sessions. The vials themselves were handled with care so as to not introduce material into the diffusion chamber that would interfere with measurements.

In order to have a controlled diffusion of the compounds from each vial, capillaries of varying dimensions were made for each compound. These were to be put through the lids on the vials. The capillaries were made from hollow glass rods, and Teflon tape and Teflon rings were used to seal and ensure minimum leakage. The capillaries were taken off and replaced by closed lids between sessions.

### 3.8 VOC emission rates

Emission rates  $r$  for the different liquid form VOCs ( $\alpha$ -pinene, toluene, m-xylene and myrcene) were tested by allowing the compounds to diffuse over time in a controlled environment, and measuring resulting weight difference. Since no emission rate was possible to get from myrcene experimentally, a probable upper and lower limit to study was extrapolated based on the other VOCs experimental values, and theoretically calculated values for all involved VOCs. Theoretically calculated rates for  $\alpha$ -pinene, toluene and m-xylene were lower than experimental rates by a factor  $\approx 3$ . Two cases were tested for myrcene, which were based on this; a lower value equal to the theoretical value; an upper value equal to roughly three times the theoretical value. This was based rather arbitrarily on the assumption that values three times the theoretical were close to the real emission rate, which was the case for the three other VOCs. These two myrcene cases would allow extrapolation of how data based on other emission rates would present itself.

The tests were performed in the main experiment set-up, but since the only variable of interest for this purpose was the  $Q_1$  flow and diffusion chamber pressure, PAM chamber UV lamps were turned off and all other flows unsupervised. Additionally the humidifier was inactive. The four vials containing  $\alpha$ -pinene, m-xylene, toluene and myrcene were placed with matching capillaries from experiments in the diffusion chamber. All procedures had to be carefully handled as the weight differences would be very small (on the order of  $10^{-2}$  g), and so even a small contamination on a vial or capillary would affect measurement. Since the only available

method of handling the vials was plastic gloves, contamination to some extent was unavoidable each weighing. The set-up was configured so that  $Q_1 = 1.5$  l/min; similar to that of during experiments, although this could vary as much as  $\pm 0.2$  l/min between measurements. The water bath was maintained at  $24 \pm 0.1$  °C and the VOCs were allowed to diffuse during a period of 25 days.

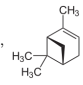
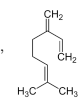
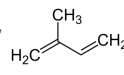
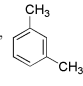
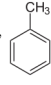
Weight was measured with an analytical balance (Mettler AT261 Delta Range), initially as well as after 12, 15 and 25 days respectively. Vials and capillaries were not de-ionized before measurement possibly adding to uncertainty. The lost weight after each measurement was then divided by the time that had passed to obtain emission rate. These intervals were considered too short to give any reliable estimate, but was subject to time constraints. The emission rate results which were used were those from the first 12 day session. Motivation for this and not taking an average was 1) Each weighing affected the results to an unknown extent, 2) Shorter diffusion sessions led to larger uncertainties, 3) Possible chemical aging of the VOCs. The other two sessions were instead used as a confirmation that the first result was reproducible.

Vapor pressure data for use in calculating eq. (6) was available from some manufacturers, but was considered too unreliable since a comparison between VOCs with this data would result in one compound having higher standard boiling point but lower vapor pressure than another. instead eq. (7) was used.

### 3.9 SMPS

The Scanning mobility particle sizer, or SMPS as it is often referred to, is a device used for measuring number size distribution of sub-micrometer particles in a gas flow. It is based on a particle's electric mobility equivalent diameter, and basically counts the number of particles of different sizes based on this for a given size interval. This equivalent diameter assumes that the measured particles are perfectly spherical, which is an approximation and not fully representative of reality. The SMPS is not able to directly weigh measured particles, but can give an approximation to this by calculating a

**Table 1:** List of the VOCs studied, as well as some basic characteristics. Since isoprene was taken from a gas tank, no vial or capillary was associated with it.

VOC	Manufacturer	Manufacturer specifications	Type	Capillaries used (Length/inner diam.)	Chemical structure
$\alpha$ -pinene	Sigma-Aldrich	(-), Fluka, analytical standard Vapor pressure: $\approx 0.4 \text{ kPa}$ (20 °C) Boiling point: 155 - 156 °C	Biogenic	7 cm / 2 mm	$\text{C}_{10}\text{H}_{16}$ , 
myrcene	Sigma-Aldrich	Technical grade Vapor pressure: $\approx 0.93 \text{ kPa}$ (20 °C) Boiling point: 167 °C	Biogenic	5 cm / 2 mm	$\text{C}_{10}\text{H}_{16}$ , 
isoprene	BOC	Gas, 1 ppm Isoprene in N <sub>2</sub> -gas Vapor pressure: $\approx 0.4 \text{ kPa}$ (20 °C) <sup>a</sup> Boiling point: 33 - 34 °C <sup>a</sup>	Biogenic	-	$\text{C}_5\text{H}_8$ , 
m-xylene	Sigma-Aldrich	puriss. p.a., $\geq 99\%$ Vapor pressure: $\approx 2.1 \text{ kPa}$ (20 °C) <sup>a</sup> Boiling point: 138 - 139 °C	Anthropogenic	7 cm / 2 mm	$\text{C}_8\text{H}_{10}$ , 
toluene	Merck	Analytical grade, $\geq 99.5\%$ Vapor pressure: $2.9 \text{ kPa}$ (20 °C) Boiling point: 110.6 °C	Anthropogenic	7 cm / 2 mm	$\text{C}_7\text{H}_8$ , 

<sup>a</sup> Value obtained from Thermodynamics Research Center (2011).

volume concentration based on measurements. This volume concentration is then assumed to be of a uniform density. Based on an average SOA density  $\rho_{soa}(\text{g cm}^{-3})$  one can then derive the mass concentration.

There are a number of factory built SMPS systems available, although the one employed in this experiment was built in-house at Lund University. The advantage over earlier systems such as the DMPS is the ability to do continuous automated scans over a desired particle size interval. With a DMPS it would be necessary to manually set each desired particle size to count. The SMPS can be simplified into its three main components; A bipolar charger; a Differential mobility analyzer or DMA, and a condensation particle counter (CPC). The CPC used in these experiments was a TSI CPC 3010 series. In reality the device is a fair bit more complex containing various sensory and regulatory equipment. Although for the purpose of this thesis, the following explanation should be sufficient.

The bipolar charger contains a radioactive material which charges incoming particles according to a well-defined charge distribution. With the particles charged, the DMA then allows particles of a certain size based on electric mobility equivalent diameter to pass. The DMA consists of two up-right concentric metal cylinders with a gap between their walls. Through the length of this gap there is a constant air flow called a sheath flow, established using a dedicated air pump. When a certain voltage is applied over the two concentric cylinders and charged particles are present in the sheath flow, the path of particles of a matching electric mobility are influenced just enough to be evacuated through a small slit in the upper end of the inner cylinder. These particles then move on to be counted by the CPC.

The CPC works by condensing a liquid (e.g. water or butanol) onto the particles, which are otherwise too small to be detected. After the particles have grown many times their original size, they are detected optically. The DMA voltage source and CPC are connected to a

computer, in the case of the Lund SMPS using software written in LabView (Roldin, 2008). This software controls a number of system parameters, such as DMA voltage which is swept over a defined corresponding size interval.

### 3.10 AMS

The AMS used in these experiments was an Aerodyne Research Inc. Aerosol Time of Flight Mass Spectrometer (ToF-AMS). (Canagaratna et al., 2007) For this thesis, its use was limited to get a preliminary SOA particle density by comparing SMPS/AMS data. By assuming that SMPS volume size distribution for one measurement interval is shifted due to each detected particle size's corresponding volume being off by a factor  $\rho_{soa}$ , one can compare with AMS mass size distribution data from the same interval, and estimate  $\rho_{soa}$ .

The ToF-AMS functions by sampling an aerosol populated air flow that is passed through an aerodynamic lens. This lens disperse a majority of the gas phase material and collimates the aerosols into a beam, which is aimed at a heated metal surface of several hundred °C. The heated surface vaporizes the particles allowing resulting vapor to be analyzed through electron ionization mass spectrometry. A rotating chopper disc is positioned between the lens and the heated surface, which blocks or allows the beam to pass. This is so that the particle size for the aerosols can be estimated by looking at particle velocities.

### 3.11 Measurements

Each experiment session was carried out continuously during one day, usually from morning to evening. A typical session lasted six to eight hours. Due to the possibility uncontrolled outside effects such as varying atmospheric air pressure affecting some flows, it was deemed advantageous to carry out sessions in as short time intervals as possible. The diffusion chamber was emptied after each session was complete to allow clean air to run through the PAM chamber, and remove any sedimented particles that could affect following measurements.

At the start of experiments, the set-up was cleared from particles to a very satisfactory de-

gree. The SMPS generally counted  $< 30$  particles  $cm^{-3}$  and a volume concentration  $< 0.01 \mu m^3/cm^{-3}$ . For all experiments the UV lamp voltage in the PAM chamber was set at  $120 \pm 3 V$ . This voltage was chosen based on tests with  $\alpha$ -pinene, where VOC mass concentration was held constant and SOA generation was tested against different voltages.  $120 \pm 3 V$  proved to give the highest SOA generation. A plot for this test can be seen in Figure 3.

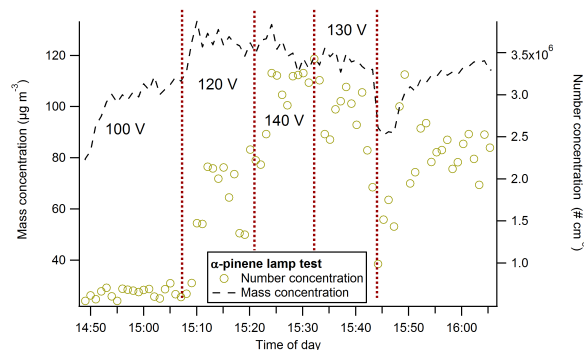


**Figure 3:** A time series depicting  $\alpha$ -pinene number and mass concentration for various lamp voltages. Values are  $\pm 3V$ .

Initially, each VOC involved in the experiments were measured by themselves. Following that, mixtures were looked at. A complete list of the experiments analyzed can be seen in Table 2. Reproducibility was tested by performing the same experiments again on days different from the first, although not for all configurations of flow  $Q_4$ . This was due to time constraints, and additionally for the very same reason, not all experiments were retried. Details on reproducibility is shown in Table 2.

All sessions started with the insertion of desired VOCs into the diffusion chamber. This was done in a fume cupboard to minimize introducing those compounds to the laboratory air. Checking and refilling water bath and humidifier water levels was also done before starting each session, as insufficient water in either systems would compromise their functionality. Neither was to be refilled during sessions; as for the water bath it would alter water temperature, and for the humidifier potentially disturb flow and RH. Following that, measurements of flows  $Q_1$ ,  $Q_2$



and  $Q_{7a}$  were made to verify that the system was properly calibrated. Diffusion chamber pressure was also measured during this time.

After the set-up was verified,  $Q_4$  was adjusted by increasing or decreasing the suction flow,  $Q_3$  in Figure 1, diverting part of the  $Q_1$  VOC flow out of the system. During adjustment, a flow meter (TSI 4100 Series) was connected in parallel with the gate valve on  $Q_4$  through the connection ports surrounding it. The gate valve was then closed to allow a complete reroute of the  $Q_4$  flow through the flow meter. This was done to minimize flow interruption while still having to connect and disconnect measurement tools.

During early experiments, it was decided that the sessions were to go from low to high VOC mass concentrations. The reasoning behind this was that a higher previous concentration would leave more VOC mass in the PAM chamber, taking longer to reach the desired mass concentration there. The  $Q_4$  flow was typically set to start at around  $0.1 \text{ l/min}$ , and was also changed in intervals of  $0.1 \text{ l/min}$ , although these parameters were varied to some degree depending on which VOCs were looked at, and what SOA volume concentration they produced. A volume concentration from  $1$  to  $100 \mu\text{m}^3 \text{cm}^{-3}$  was aimed for in order to simulate atmospheric conditions, although that limit couldn't always be reached for some VOCs with this set-up. It took between  $10 - 30$  minutes for the PAM chamber to reach a stable SOA production from each VOC mass concentration that was input. Exceptions to this were some experiments, such as the ones containing myrcene which could take as much as up to  $1.5$  hours to reach stable levels.

An example of SMPS data from one experiment session is shown in Figure 4. Tenax sample collection was used for all experiments, although generally only three to four samples were taken. These were pipes containing the material Tenax, which collected the gas mass to be analyzed in a mass spectrometer. Priority for these samples were given to low VOC mass concentrations, i.e. at low  $Q_4$  flows, since the concentrations would be most uncertain there.

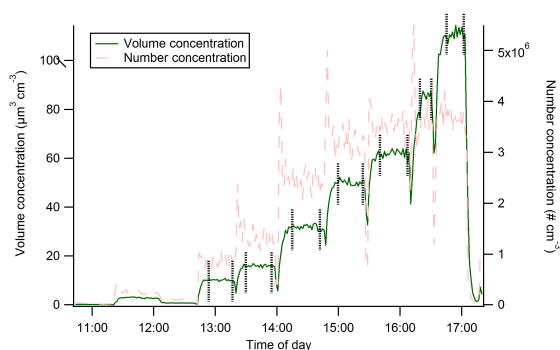


**Figure 4:** Example of SMPS data from an experiment with myrcene, *m*-xylene & *a*-pinene. Dashed vertical lines show the intervals which were of interest.

## 3.12 Data analysis

### 3.12.1 SOA yields

The SOA yields were calculated for all experiments with individual VOCs, as well as the experiments with VOC mixtures. For all calculations converting SMPS SOA volume concentration to mass concentration, a density of  $1.4 \mu\text{g cm}^{-3}$  was used, based mainly on data from Kuwata et al. (2012), as well as other studies verifying similar results (Shilling et al., 2008; Ng et al., 2007; Nakao et al., 2013).

A script was constructed in MATLAB to analyze SMPS data from each experiment session. The relevant data was of measured SOA volume concentration for each VOC mass concentration level that was reacted in the PAM chamber. This data was the plateau data of which an example is shown in Figure 4. The code for this script can be found in appendix A. The script would display the volume concentration plateau data for selected experiment and give the user ability to select intervals in which the arithmetic average, standard deviation, volume and number size distribution would then be calculated. For ease of work, the script was made so that each processed interval and all calculated data could be saved with a customizable tag to the MATLAB workspace.

Since each new VOC mass concentration setting required some time for SOA production to reach an equilibrium (usually between  $10 - 20$  minutes), the left-hand side of each interval

had to be carefully chosen. The interval average would then be inserted into an Excel sheet and paired with other relevant data for each plateau, such as  $O_3$  levels,  $Q_1$ ,  $Q_2$ ,  $Q_4$  flows and emission rate  $r$   $\mu g/min$  for each VOC and accompanying capillary present in the experiment. These data sheets are available in Appendix B.

An estimation of the mass concentration for each involved VOC was then calculated based on  $Q_1$ ,  $Q_2$ ,  $Q_4$  ( $l/min$ ), and  $r$  ( $\mu g/min$ )

$$\Delta HC = \frac{r}{Q_1 * 10^{-3}} * \frac{Q_4}{Q_2 + Q_4} (\mu g/m^3) \quad (14)$$

where the left multiplicative term represents the VOC mass concentration in  $Q_1$  and  $Q_4$ ; The right multiplicative term the fraction of VOC mass concentration after  $Q_4$  and  $Q_2$  have converged and mixed.

For a VOC mixture,  $\Delta HC$  would simply be calculated as the sum of the individual VOC mass concentrations

$$\Delta HC = \Delta HC_{VOC,1} + \Delta HC_{VOC,2} + \dots + \Delta HC_{VOC,N}. \quad (15)$$

The SOA mass concentration was then calculated based on measured volume concentration, and divided by the total VOC mass concentration according to eq. (8).

### 3.12.2 Two-product model comparison

The purpose of this comparison was to see if the SOA yield of a VOC mixture corresponded well with a theoretical linear approximation of its yield. The idea was to use data from individual VOC measurements, and build a linear approximation for mixtures based on this. This was done by employing the absorptive gas-particle partitioning model eq. (10) laid out by Pankow (1994*b,a*); Odum et al. (1996), which in this paper is referred to as the two-product model. This would be the method in which this thesis explored possible non-additive yield results.

Corresponding two-product model constants

were approximated for each experimental SOA yield curve where  $\alpha$ -pinene, myrcene, m-xylene, toluene and isoprene had been measured independently. This was done using MATLAB's curve fitting tool `cftool` with the two-product model equation eq. (10). A legacy version of this tool had to be used, accessed with the command `cftool -v1` as the current version (MATLAB R2013a) had issues handling custom non-linear equations with multiple unknown constants.

The curve was fitted for experimental yield data by finding good values for the equation constants  $\alpha_{1,2}$ ,  $k_{om,1,2}$ . Good values were considered to be  $0 < \alpha_{1,2} < 1$ , and  $0 < k_{om,1,2} < 5$ . These limits were somewhat arbitrarily chosen based on results from other studies<sup>2</sup>. As limiting intervals were set for sought constants, a trust-region algorithm was employed.

These two-product models were then used for each mixture to compare with experimental measurements of the same mixture.

### 3.13 Uncertainty limits

Uncertainty limits for experimental measurements was narrowed down to three factors; i) Uncertainty in air flow measurement readings for VOC mass concentration estimations, ii) Uncertainty in recorded SMPS volume concentration, iii) Uncertainty in emission rates. All of these points were of direct influence in the calculated VOC mass concentration. In reality there were more uncertainties, but these were the ones significant and tangible enough to work with in the given time frame with given materials. Other uncertainty sources were: room temperatures, atmospheric pressures, fluctuating voltage on UV lamps, VOC vials changing chemical composition/becoming contaminated over time, diffusion chamber temperature, needle valve flow settings.

i) The flow meter used was of model TSI 4100 series. Manufacturer specifications claim that for measurement in air or oxygen, the maximum error of the device is 2 % of reading, with a minimum of 0.005 l/min at 21.1 °C, 101.3 kPa. For each degree away from 21.1 °C, 0.075 % was to be added to the error, and for every

<sup>2</sup>e.g. Odum et al. (1996); Ng et al. (2007); Shilling et al. (2008)

kPa above 101.3 kPa 0.015 % was to be added to the error. Certain flows in the experiment setup were at 24 °C, and average pressure in the diffusion chamber was 105.8 kPa. These values were chosen to represent the system, and resulted in a flow error of 2.3 %, with a minimum error of 0.005 *l/min*. This was then applied on all measured flows in such a way that a minimum and maximum could be obtained .

Flow data was mainly relevant to calculate VOC mass concentrations described by eq. (14). In order to get maximum/minimum representation of these uncertainties, two cases were explored. Each with a configuration of  $Q_4 \pm e$ ,  $Q_1 \pm e$ ,  $Q_6 \pm e$  ( $Q_{iso} \pm e$ ) in such a way that would yield the largest/smallest value.  $e$  denotes error.

ii) The SMPS data collected volume concentration information once every minute while running. Because an average session for each VOC mass concentration level studied was around 30 - 40 minutes, and about 10 minutes of that time was needed for equilibrium to be achieved, about 20 - 30 data points would be collected on average. From this data mean and related standard deviation was calculated with MATLAB. Values can be seen in appendix B.

iii) VOC emission rates were examined by means of weight difference under a 25 day diffusion session, during which VOC vials were weighed a total of four times. This was much too short to give reliable data, and any weighing increased uncertainties due to possible contamination. Emission data from the longest interval under these 25 days was used, with the other intervals only verifying that a consistent pattern could be observed. No fluctuation larger than 25 % was observed in these tests.

Data from previous PTR-MS measurements with  $\alpha$ -pinene, with the same diffusion chamber set-up as in main experiments, were analyzed in order to get a reasonable uncertainty limit from emission rate. This data only contained three tests that had been made with  $\alpha$ -pinene and matching capillary, so also here there is large uncertainty. Two of the tests also included  $\beta$ -caryophyllene in the diffusion chamber, although it was judged that this wouldn't influ-

ence  $\alpha$ -pinene results. The three data points had been taken during intervals of 1, 1.5 and 11 hours. During the 11 hour interval, only a fluctuation of  $\approx 7$  % was observed. Between the mean of the two longest intervals, which were separated by three days, only a difference of 1.6 % was observed. Because of these results, an uncertainty of 6 % was set for emission rates. This is with most certainty an underestimation.

## 4 Results & discussion

### 4.1 SOA yields

A summary of all experiments can be seen in Table 2. The two-product model constants used can be viewed in Table 3. Uncertainties are presented more in depth in section 3.13. Consistent emission rates from weighing tests were obtained for all VOCs except myrcene. Experimental and theoretical emission rates can be seen in Table 4. Myrcene instead showed a non-consistent increase in mass over time during diffusion tests. This was possibly from chemical interaction with the other compounds present in the diffusion chamber, although the real reasons are unknown. An upper and lower case was instead used for myrcene.

SOA density was calculated to  $\rho_{soa} = 2.0 \text{ g cm}^{-3}$ . This was based on AMS-SMPS average size distribution data analysis for the two highest  $\Delta HC$  levels, done on experiments [ $\alpha$ -pinene], [m-xylene], [ $\alpha$ -pinene], [myrcene, m-xylene,  $\alpha$ -pinene]. Although this density might be of interest, it was not used in estimating SMPS SOA mass in this study. This since AMS data was not properly calibrated, and  $\rho_{soa} = 2.0 \text{ g cm}^{-3}$  is not a reliable estimate. Instead a density of  $\rho_{soa} = 1.4 \text{ g cm}^{-3}$  was used, based on findings from other studies (Kuwata et al., 2012; Shilling et al., 2008; Ng et al., 2007; Nakao et al., 2013).

The yield results for  $\alpha$ -pinene and m-xylene, assuming a SOA density of  $1.4 \text{ g cm}^{-3}$  are comparable to values obtained by Kang et al. (2011) and Ng et al. (2007), depicted in Table 5.

The experiments of Kang et al. (2011) were as with this study performed with a PAM chamber, and  $\alpha$ -pinene results compare very well to

**Table 2:** Summary of the performed experiments. Times performed indicated number of times repeated / within what average accuracy those repetitions were. VOC and SOA mass concentrations are presented as lowest - highest values from the measurement series, with uncertainty included for the highest. Difference from model yield is an average of all points. For yield, only the value corresponding to highest VOC reacted mass concentration is shown.  $O_3$  range is the recorded changes in PAM chamber ozone levels during each experiments.

Experiment		Times performed/ Accuracy	$\Delta HC$ range ( $\mu g/m^3$ )	$M_0$ range ( $\mu g/m^3$ )	$O_3$ range (ppb)	Difference from two-product model ( $Y/Y_{2p}$ )	Yield (%)
VOC	Mixture ratios						
$\alpha$ -pinene		3 / 20 %	29 - 179 $\pm$ 11	1.8 - 101 $\pm$ 1.4	5800 - 6260	-	40 $\pm$ 6.1%
m-xylene		2 / 30 %	47 - 291 $\pm$ 17	0 - 57 $\pm$ 1.6	5580 - 6120	-	14 $\pm$ 2.4%
myrcene		1 / - %	20 - 117 $\pm$ 7	0 - 27 $\pm$ 0.8	4510 - 5560	-	17 $\pm$ 1.4% / 50 $\pm$ 3.9%
isoprene		1 / - %	45 - 510 $\pm$ 31	0 - 2.7 $\pm$ 0.1	5480 - 6190	-	0.3%
toluene		1 / - %	66 - 746 $\pm$ 45	1.5 - 188 $\pm$ 3.0	4910 - 5360	-	18 $\pm$ 2.9%
$\alpha$ -pinene m-xylene	(39%) (61%)	1 / - %	43 - 402 $\pm$ 24	0.4 - 150 $\pm$ 2.8	5430 - 6130	-9 %	27 $\pm$ 4.3%
m-xylene isoprene	<sup>a</sup> (16 $\rightarrow$ 59%) (84 $\rightarrow$ 41%)	1 / - %	246 - 423 $\pm$ 26	0.4 - 37 $\pm$ 1.1	5000 - 5270	-4 %	9 $\pm$ 1.1%
$\alpha$ -pinene toluene	(10%) (90%)	1 / - %	42 - 825 $\pm$ 50	0.3 - 235 $\pm$ 4.6	5430 - 6130	-4 %	20 $\pm$ 3.4%
myrcene m-xylene	<sup>b</sup> (12/29%) (88/71%)	1 / - %	29 - 271 $\pm$ 16 / 36 - 335 $\pm$ 20	0.5 - 111 $\pm$ 2.8	5160 - 5590	30 % / 30 %	26 $\pm$ 5.0% / 21 $\pm$ 4.1%
myrcene m-xylene $\alpha$ -pinene	<sup>b</sup> (8/20%) (57/49%) (35/31%)	1 / - %	22 - 328 $\pm$ 20 / 25 - 379 $\pm$ 23	0.1 - 156 $\pm$ 3.0	4530 - 5470	12% / 12%	34 $\pm$ 5.5% / 29 $\pm$ 5.9%
myrcene m-xylene $\alpha$ -pinene isoprene	<sup>c</sup> (1 $\rightarrow$ 4%/2 $\rightarrow$ 12%) (4 $\rightarrow$ 32%/2 $\rightarrow$ 30%) (3 $\rightarrow$ 20%/3 $\rightarrow$ 19%) (92 $\rightarrow$ 43%/91 $\rightarrow$ 39%)	1 / - %	240 - 501 $\pm$ 30 / 237 - 461 $\pm$ 28	2 - 150 $\pm$ 3.2	5050 - 5330	16% / 16%	23 $\pm$ 2.9% / 21 $\pm$ 2.7%

<sup>a</sup> Due to constant isoprene VOC mass concentrations, ratios changed during experiment. This is shown with an arrow going from initial to final value.

<sup>b</sup> For mixes including myrcene, scenarios corresponding to  $r_{myrc} = 0.3/r_{myrc} = 0.9$  ( $\mu g/min$ ) are shown throughout table.

<sup>c</sup> As both isoprene and myrcene were present, two scenarios representing changing mixture ratios are shown.

**Table 3:** Two-product constants used in these experiments.

VOC	$\alpha_1$	$\alpha_2$	$k_{om,1}$	$k_{om,2}$
This study				
$\alpha$ -pinene	0.0617	0.4788	0.4814	0.03507
m-xylene	0.0871	0.476	0.1267	0.003886
toluene	0.01823	0.2336	0.8908	0.04462
myrcene, $r = 0.3$	0.08894	0.8613	1.100	0.04851
myrcene, $r = 0.9$	0.03106	0.2883	1.009	0.04737
isoprene	0.002131	0.06325	0.8419	0.02074

these. For m-xylene there is about a factor 2 difference in yield. This would most likely be due to differences in relative humidity and OH concentration.

#### 4.1.1 $\alpha$ -pinene & m-xylene

The mixture showed a final  $27 \pm 1.7$  % SOA yield, visible in Figure 5. This yield was on average 9 % lower than a comparison with the constructed two-product model of the mixture. The two-product models for the individual VOCs as well as the experimental data which they were based on can be viewed in Figure 6.

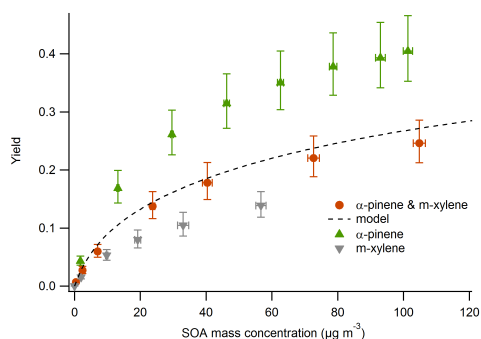


**Figure 5:** Yield curve for the experimental and two-product model SOA yields for the [ $\alpha$ -pinene, m-xylene] mixture. The yields from measurements with the individual VOCs are also shown, from which the mixture model yield was derived. Notably these individual measurements didn't reach as high in SOA mass concentrations as the mixture itself, adding to uncertainty for values beyond that.

The model was most accurate for mass concentrations  $< 60 \mu\text{g}/\text{m}^3$  due to the experiments with m-xylene not going further. Within that region the difference was less than 5 %. Beyond  $60 \mu\text{g}/\text{m}^3$  the uncertainty of m-xylene yield gets large, and so it's entirely possible that the model yield is within the accuracy of measurements. This is further strengthened by established error limits. The two-product model was extrapolated from the measurements of the individual VOC components, and neither of those explored as high SOA mass concentrations as the mixture, affecting the accuracy of the two-product model constants obtained by curve fitting. The number of measurement points is also relevant for a good curve fit, and for both  $\alpha$ -pinene and m-xylene relatively few (eight

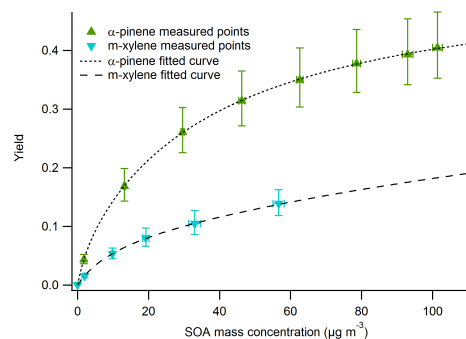


**Figure 6:** The experimental data compared to the two-product model curve fit for  $\alpha$ -pinene and m-xylene. The coefficients are  $\alpha_1: 0.0617$ ,  $k_{om,1}: 0.4814$ ,  $\alpha_2: 0.4788$ ,  $k_{om,2}: 0.03507$  and  $\alpha_1: 0.0871$ ,  $k_{om,1}: 0.1267$ ,  $\alpha_2: 0.476$ ,  $k_{om,2}: 0.003886$  for  $\alpha$ -pinene and m-xylene respectively. The curve fits follow the experimental data well, but as in the case of m-xylene, there is a larger uncertainty for SOA mass concentration  $> 60 \mu\text{g cm}^{-3}$ , which would be inherited by any use of the model beyond that. This is also true for  $\alpha$ -pinene SOA mass concentration  $> 105 \mu\text{g cm}^{-3}$ .

and six respectively) were taken, adding to uncertainty.

As can be seen in Figure 5, the mixture of  $\alpha$ -pinene and m-xylene never reached high enough concentration pre-PAM to enable a definitive leveling out of the yield curve. Because of this the final yield is most likely higher than the measured  $27 \pm 4.5$  %. In Figure 7, the growth curve for the mixture show a near-linear relation between SOA and VOC mass concentration in the VOC mass concentration interval  $100 - 400 \mu\text{g}/\text{m}^3$ .

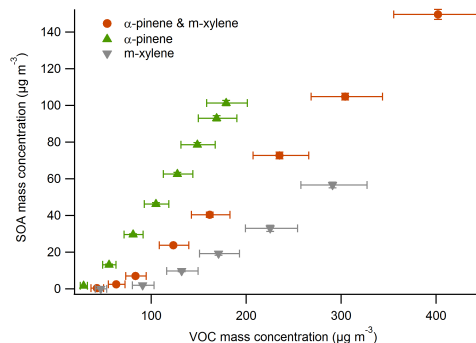


**Figure 7:** Growth curve for the [ $\alpha$ -pinene, m-xylene] mixture as well as  $\alpha$ -pinene and m-xylene individually.

Due to the higher emission rate and concentration of m-xylene in this mixture, the mixture growth curve is gravitating somewhat towards m-xylene.

**Table 4:** Emission rates for the four liquid form VOCs used in this study. Except for myrcene, experimentally obtained numbers were the ones used for estimating VOC mass concentrations from the experiments. Motivation for using a  $\pm 6\%$  uncertainty for the values is detailed in section 3.13.

VOC	Emission rate, $r$ ( $\mu\text{g min}^{-1}$ )		
	experimental	theoretical	used in this study ( $\pm 6\%$ )
$\alpha$ -pinene	1.4	0.49	1.4
m-xylene	2.2	0.87	2.2
toluene	12	2.9	12
myrcene	-	0.31	0.3 / 0.9

**Table 5:** Yield comparison with other studies for  $\alpha$ -pinene and m-xylene. The higher m-xylene yield of this study could be due to differing OH concentration and RH.

VOC	Reference	$\Delta\text{HC}$ ( $\mu\text{g m}^{-3}$ )	OH exposure (molecules $\text{cm}^{-3}\text{s}$ )	RH (%)	$M_0$ ( $\mu\text{g m}^{-3}$ )	SOA Yield (%)
$\alpha$ -pinene	This work	$179 \pm 11$	$\approx 7 * 10^{11}$	$30.6 \pm 0.3$	$101 \pm 1.4$	$40 \pm 6.1$
	Kang et al. (2011)	$217 \pm 33$	$(2.8 \pm 0.9) * 10^{11}$	<sup>a</sup>	$110 \pm 10$	$54 \pm 10$
	Kang et al. (2011)	$217 \pm 33$	$(7.8 \pm 2.5) * 10^{11}$	<sup>a</sup>	$110 \pm 10$	$52 \pm 9$
	Kang et al. (2011)	$217 \pm 33$	$(1.3 \pm 0.5) * 10^{12}$	<sup>a</sup>	$94 \pm 9$	$45 \pm 8$
	Kang et al. (2011)	$217 \pm 33$	$(2.3 \pm 0.8) * 10^{12}$	<sup>a</sup>	$94 \pm 9$	$45 \pm 8$
	Ng et al. (2007)	$264 \pm 4$	-	6.2	$121.3 \pm 9.4$	$45.8 \pm 3.6$
m-xylene	This work	$291 \pm 17$	$\approx 7 * 10^{11}$	$30.6 \pm 0.3$	$57 \pm 1.6$	$14 \pm 2.4$
	Kang et al. (2011)	$737 \pm 130$	$(6.2 \pm 4.0) * 10^{11}$	<sup>a</sup>	$63 \pm 7$	$9 \pm 2$
	Kang et al. (2011)	$737 \pm 130$	$(1.2 \pm 0.5) * 10^{12}$	<sup>a</sup>	$53 \pm 7$	$7 \pm 2$
	Kang et al. (2011)	$737 \pm 130$	$(1.9 \pm 0.9) * 10^{12}$	<sup>a</sup>	$52 \pm 7$	$7 \pm 2$
	Kang et al. (2011)	$737 \pm 130$	$(2.4 \pm 0.8) * 10^{12}$	<sup>a</sup>	$57 \pm 7$	$8 \pm 2$

<sup>a</sup>The RH levels of the Kang et al. (2011) experiments is stated as varying between 3 - 45 %.

Number and mass size concentrations for the mixture are shown in Figure 8 and 9. These distributions are taken from the highest measured  $\Delta\text{HC}$  point in each experiment. Corresponding VOC or SOA mass values can be seen in Table 2. The majority of particles for all subjects lie in the nucleation mode, although all three also show small tops in the Aitken mode.

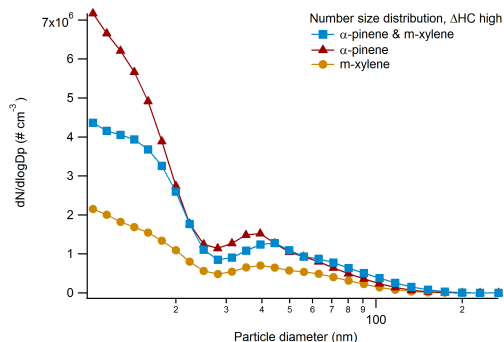


**Figure 8:** Number size distribution at highest  $\Delta\text{HC}$  for the [ $\alpha$ -pinene, m-xylene] mixture and individual VOCs. Lines between points are present to help guide the eye.

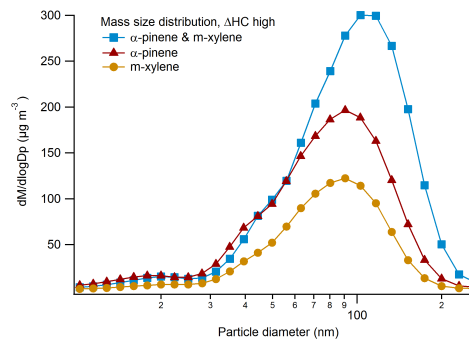


**Figure 9:** Mass size distribution at highest  $\Delta\text{HC}$  for the [ $\alpha$ -pinene, m-xylene] mixture and individual VOCs. Lines between points are present to help guide the eye.

Instead looking at mass, almost all mass lie on the border to the accumulation mode, with a small but noticeable bump in the Aitken mode. No non-additive indications can be seen here, since VOC mass concentrations of  $\alpha$ -pinene and m-xylene are rather similar between the mixture and plotted individual ones and the resulting SOA mass seem to be roughly additive. It is interesting to note that the mixture mass top is shifted slightly toward the right.

### 4.1.2 m-xylene & isoprene

The flow of isoprene was held constant throughout the measurement. Since VOC flow  $Q_4$  was to be varied, a constant isoprene flow was preferred and set to  $0.5 \text{ l/min}$  representing a VOC mass concentration of roughly  $200 \mu\text{g}/\text{m}^3$ . This meant that total mixture ratios would change depending on  $Q_4$  setting. The mixture showed a  $9 \pm 1.1 \%$  yield, but as can be seen in Figure 10 the curve is far from leveling out.

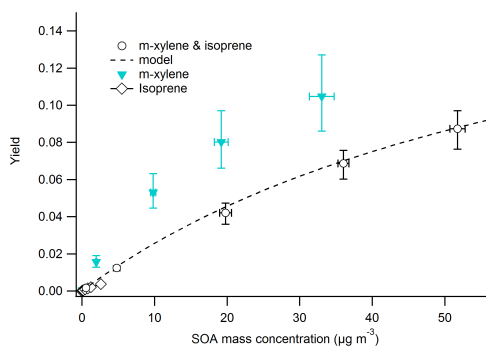


**Figure 10:** Yield curve and model for m-xylene and isoprene mixture. Also shown is the experimental data for individual VOCs which the model is based on. Note how the model follows the data rather closely.

The experimental yield is furthermore 4% lower than corresponding two-product model prediction, and seem to follow the two-product model well. It is possible though that the experimental data would surpass the model for SOA mass concentrations  $> 60 \mu\text{g cm}^{-3}$ , as the model seem to level out at a faster rate relative to the measurements. However, very little can be said about this without further experiments. Looking at Figure 11, the very low SOA mass concentrations achieved with isoprene makes for a large uncertainty in how its yield actually propagates at larger mass concentrations, and it's entirely possible that the good yield/model match is a coincidence. No growth curve was made with isoprene data due to the constant isoprene VOC mass concentrations. Since it was independent of  $Q_4$  setting, it shifted the isoprene curve and made it difficult to present any useful data.

In Figure 12, one can see a pattern similar to that of the mixture in Figure 8. Here the nucleation mode and two Aitken mode bumps are visible.

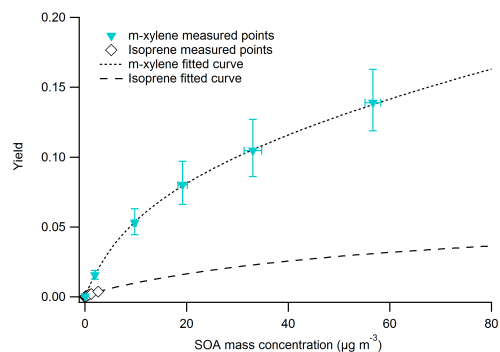


**Figure 11:** The yield curves derived from the two-product model, with measurement data for reference. Notice the very long extrapolation for isoprene. Parameters used for isoprene were  $\alpha_1: 0.002131$ ,  $k_{om,1}: 0.8419$ ,  $\alpha_2: 0.06325$  and  $k_{om,2}: 0.02074$ . Lines between points are present to help guide the eye.

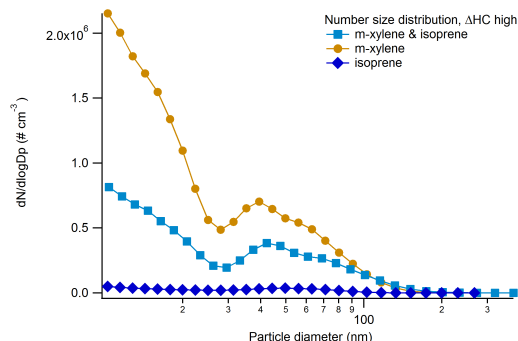


**Figure 12:** Number size distribution at highest  $\Delta HC$  for the [m-xylene, isoprene] mixture and individual VOCs. Lines between points are present to help guide the eye.

$\Delta HC$  for isoprene in the presented distribution was around  $500 \mu\text{g m}^{-3}$ , while the mixture was only  $420 \mu\text{g m}^{-3}$ . Isoprene as in Figure 8 seemed to suppress nucleation mode particles, although this didn't seem to have an effect on resulting yield. Again the mixtures mass size distribution seen in Figure 13 is shifted to the left, and some notice of Aitken mode activity exists on both the mixture and m-xylene curve. Again no obvious non-additivity was seen in the size distributions.

### 4.1.3 Myrcene & m-xylene

Since no reliable experimental emission rate was found for myrcene, a lower case equal to the theoretically calculated  $r_{myrc} = 0.3 \mu\text{g}/\text{min}$ , and an upper case  $r_{myrc} = 0.9 \mu\text{g}/\text{min}$  was looked

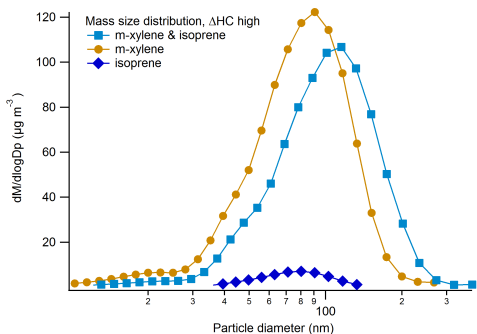


**Figure 13:** Mass size distribution at highest  $\Delta HC$  for the [m-xylene, isoprene] mixture and individual VOCs. Here one again can see the the mixture having shifted to the right towards the accumulation mode.

at.  $r_{myrc} = 0.9 \mu g/min$  was considered to lie close to the actual emission rate, but this could not be confirmed. As a result there are very large uncertainties in these experiments, but as a preliminary approach it has some value.

Yield results can be seen in Figure 14. The mixture showed a yield of  $26 \pm 5.0\%/21 \pm 4.1\%$  for  $r_{myrc} = 0.3/0.9 \mu g m^{-3}$  respectively. Here experimental yield is for all points larger than their corresponding two-product model, on average differing with 29% for the last five data points.

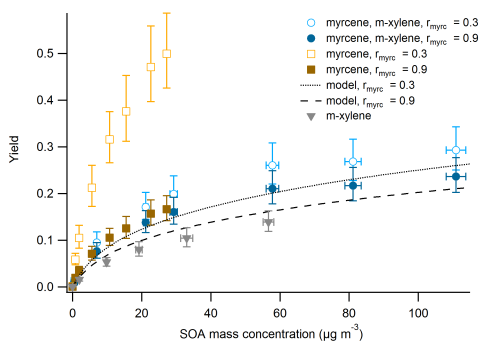


**Figure 14:** Yield diagram for the [myrcene & m-xylene] mixture. Shows two sets of curves for experiments involving myrcene, exploring different emission rates for myrcene as they are unknown. Also shows the individually experimental yields for m-xylene and myrcene.

For neither r-case does the model fall within established error limits. Individual myrcene yield is very different depending on case; 50% for  $r_{myrc} = 0.3$  and 17% for  $r_{myrc} = 0.9$ , although only affecting mixture yield marginally due to its low

mixture fraction. On average the experimental yield is 30%/30% higher compared to two-product models. It is possible that the experimental yield would converge on the model yield for SOA mass concentrations  $> 110 \mu g cm^{-3}$  although considering the large uncertainties involved, more experiments would be required to confirm so. On a very preliminary basis it is possible that some yield-affecting mechanism not considered by the two-product model occurs. The uncertainty of myrcene emission shouldn't be contributing to a significant difference in yield as long as r-values are within probable limits. The mixture growth curve can be seen in Figure 15.

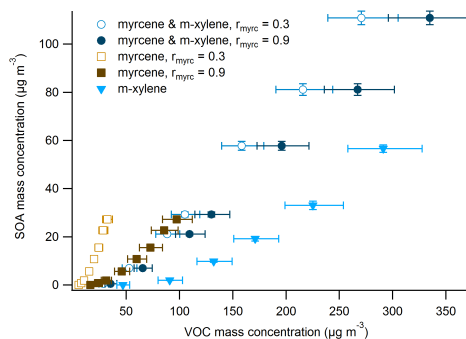


**Figure 15:** Growth diagram for the [myrcene & m-xylene] mixture for  $r_{myrc} = 0.3 \mu g/min$  and  $r_{myrc} = 0.9 \mu g/min$ .

As can be viewed in Figure 16, there was a slight shift of the mixtures mass top towards lower diameters.

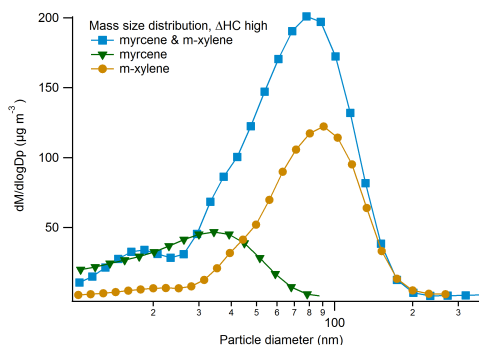


**Figure 16:** Mass size distribution at highest  $\Delta HC$  for the [myrcene, m-xylene] mixture and individual VOCs. Lines between points are present to help guide the eye.

Myrcene number concentrations seen in Figure 17 were very high, to such an extent that the



CPC had problems counting. This wasn't viewed as a big issue, as the slopes of the distributions did seem to follow good and continuous patterns.

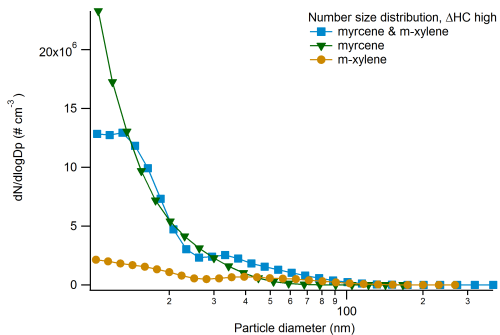


**Figure 17:** Number size distribution at highest  $\Delta HC$  for the [myrcene, m-xylene] mixture experiment as well as individual VOC experiments. One can see that the number concentration for the mixture be clearly cut-off at around  $13 \times 10^6 \text{ cm}^{-3}$  after having followed the myrcene concentration curve quite well. This is possibly a CPC issue, which had problems counting such large number concentrations. Lines between points are present to help guide the eye.

It was noted that while the mixture again was on the border between Aitken mode and accumulation mode, myrcene stayed completely in the nucleation and Aitken mode. It is possible that this is what's causing there to be no mass top shift towards higher diameters in the mass size distribution for the mixture.

#### 4.1.4 Myrcene, m-xylene & $\alpha$ -pinene

As with the myrcene & m-xylene experiment, the same two cases for the unknown myrcene emission rate were used as to try and give an estimation of probable values. The results can be seen in Figure 18.

With the addition of  $\alpha$ -pinene in the diffusion chamber, the two cases of experimental mixture yields both seemed to follow their corresponding two-product model curves well, and for both cases experimental yield was on average 12% higher than model yields. Each model curve was also well within the error limits for all experimental yield points. Experimental yields were  $34 \pm 5.5\%/29 \pm 5.9\%$  for  $r_{myrc} = 0.3/0.9 \mu\text{g}/\text{min}$ , respectively. The reason for this large difference in two-product model compatibility compared to the myrcene & m-xylene mix is unclear.

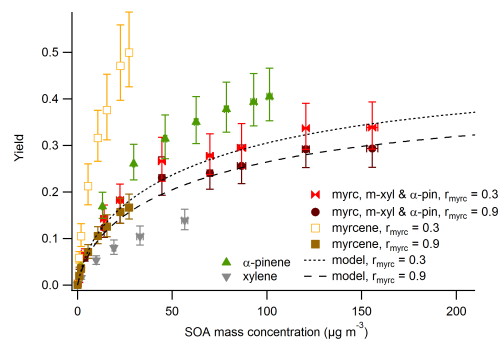


**Figure 18:** Yield diagram for the [myrcene, m-xylene and  $\alpha$ -pinene] mixture experiment for the two  $r_{myrc}$  scenarios. Note how well experimental values follow corresponding two-product model.

When looking at the growth curve for the mixture (Figure 19), it can be seen that the mixture growth lies very close to myrcene for  $r_{myrc} = 0.9$ .

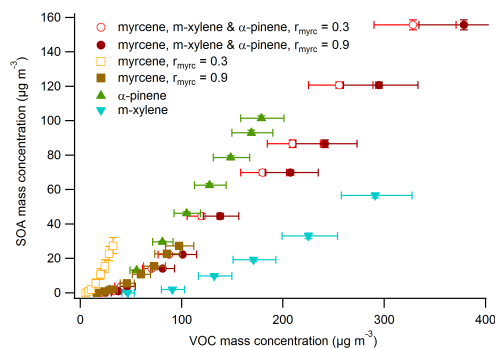


**Figure 19:** Growth diagram for the [myrcene, m-xylene &  $\alpha$ -pinene] mixture. Here the two  $r_{myrc}$  mixture scenarios lie fittingly between its VOC components.

This is very similar to the experiment without  $\alpha$ -pinene shown in Figure 15, for both  $r$ -cases despite the added  $\alpha$ -pinene which constitute a large fraction of the mixture and has a high SOA yield. Number and mass size distributions can be viewed in Figure 20 and Figure 21 respectively.

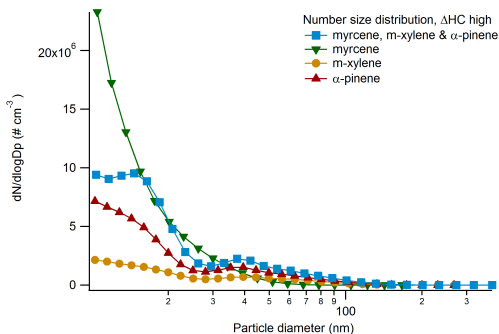


**Figure 20:** Number size distribution at highest  $\Delta HC$  for the [myrcene, m-xylene,  $\alpha$ -pinene] mixture experiment as well as individual VOC experiments. One can see the number concentration for the mixture is clearly cut-off at around  $13 \times 10^6 \text{ cm}^{-3}$  after having followed the myrcene concentration curve quite well. This is possibly a CPC issue, which had problems counting such large concentrations. Lines between points are present to help guide the eye.

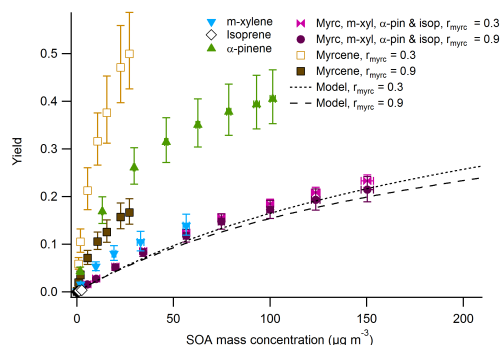


**Figure 22:** Yield diagram for the [myrcene, m-xylene,  $\alpha$ -pinene] & isoprene mixture. Also shown are the two-product models for the two  $r_{myrc}$  cases, as well as the individual mixture VOC component yields.

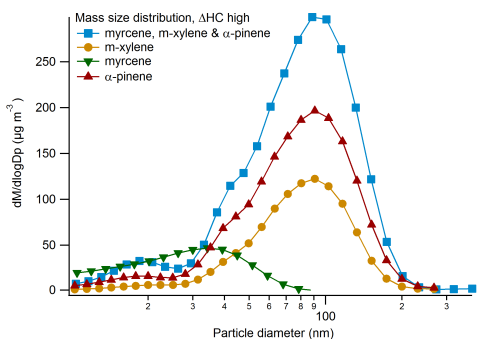


**Figure 21:** Mass size distribution at highest  $\Delta HC$  for the [myrcene, m-xylene,  $\alpha$ -pinene] mixture and individual VOCs. Lines between points are present to help guide the eye.

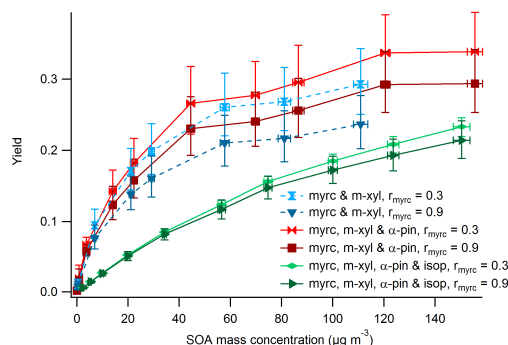


**Figure 23:** Yield diagram for all three myrcene containing mixture experiments. Lines are drawn between measurement points to help guide the eye and allow for easier comparison. Notice the deviating shape and steadier measurement points of the mixture containing isoprene.

### 4.1.5 Myrcene, m-xylene, $\alpha$ -pinene & isoprene

Adding isoprene to the mixture, one could see a rather large decrease in experimental yield from the mixture without isoprene. The result is seen in Figure 22. The resulting yield was  $23 \pm 2.9\% / 21 \pm 2.7\%$  for  $r_{myrc} = 0.3$  and  $r_{myrc} = 0.9$  respectively. A similar decrease was also seen in the m-xylene & isoprene mixture experiment compared to m-xylene alone. It is not totally unexpected con-

sidering the large mass concentration of isoprene used, coupled with its low yield. What is of interest though is how isoprene seem to stretch out the yield curve and slow down the yield increase, more clearly visible in Figure 23.

Comparing the [myrcene, m-xylene] experiment with the [myrcene, m-xylene,  $\alpha$ -pinene] experiment, one can deduce a roughly similar point of the yield curves leveling out, while the experiment with added isoprene has a much slower, steadier growing curve. It is possible that this curve at high enough SOA mass concentrations would end up higher than the non-isoprene counterpart as seen in Figure 24, but that would require further experiments to determine. In Figure 22, it's again noticeable that the experimental yield does not

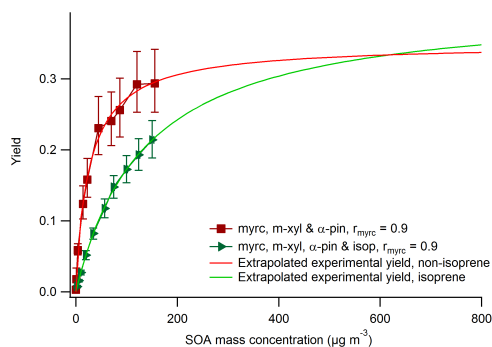


**Figure 24:** Extrapolated yield diagram for [myrcene, m-xylene, alpha-pinene] mixture with and without isoprene. Based on two-product approximations derived directly from mixture experimental results. At a SOA mass concentration of around  $600 \mu\text{g m}^{-3}$ , the isoprene mixture surpasses the non-isoprene mixture.

match the two-product models theoretical yield. The difference between experimental and model yield were 16% for both myrcene cases, but it is again a large uncertainty in the mixture model yield due to the large extrapolation of the isoprene model yield curve, shown in Figure 11.

The number and mass size distributions, shown in Figure 25 and Figure 26 respectively, for the highest measured level of  $\Delta HC$  was in general very similar to those of previous myrcene mixtures.

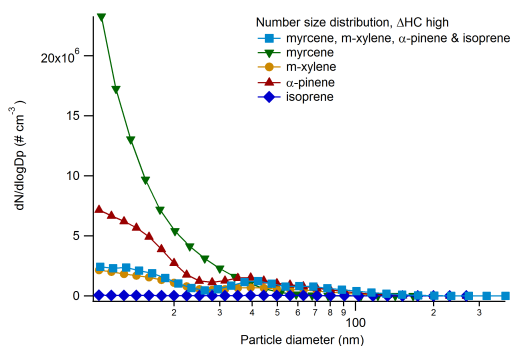


**Figure 25:** Number size distribution at highest  $\Delta HC$  for the [myrcene, m-xylene, alpha-pinene] mixture experiment as well as individual VOC experiments. Lines between points are present to help guide the eye.

The strong effect isoprene had on nucleation mode particles in the mixture was again observed, but what was interesting was that there was again a shift in the mass top for the mixture previously seen in the [m-xylene, isoprene] mixture, and to

some extent in the [ $\alpha$ -pinene, m-xylene] mixture. It is possible that isoprene is involved in this shift, as they were not observed in other myrcene mixtures. It's difficult to speculate about as a much more coherent approach is needed, not least in seeing to that  $\Delta HC$  levels for the experiments are relevant for comparison. Again no non-additive effects could be deduced from this data.

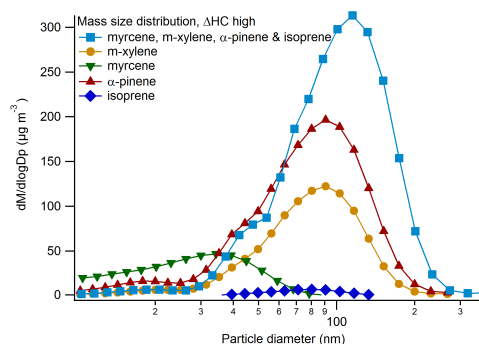


**Figure 26:** Mass size distribution at highest  $\Delta HC$  for the [myrcene, m-xylene, alpha-pinene] mixture and individual VOCs. Lines between points are present to help guide the eye.

#### 4.1.6 Toluene & $\alpha$ -pinene

Experimental yield of the mixture was  $20 \pm 1.4\%$ . This is only about 2 % higher than results from individual toluene aging experiments. With toluene's large emission rate at  $12 \mu\text{g}/\text{min}$ , it was difficult to set up a good mixture ratio between it and  $\alpha$ -pinene through the use of capillaries. As can be seen in Table 2, the mixture consisted to 90 % of toluene. It was because of this expected to see a resulting yield dominated by toluene's properties. The result was an experimental yield 4 % lower than corresponding model yield. As can be seen in Figure 27, the model yield curve lies just inside error limits for the mixture. Since the mixture ratio was also very toluene dominated, it would be more difficult to detect effects other than what the two-product model can predict.

The [toluene,  $\alpha$ -pinene] mixture number size distribution shown in Figure 28, for the highest  $\Delta HC$  level ( $825 \pm 50$ ,  $750 \pm 45$  and  $180 \pm 11 \mu\text{g m}^{-3}$  for mixture, toluene and  $\alpha$ -pinene respectively) was very similar to previous distributions, with a majority of nucleation mode particles and some Aitken mode particle tops.

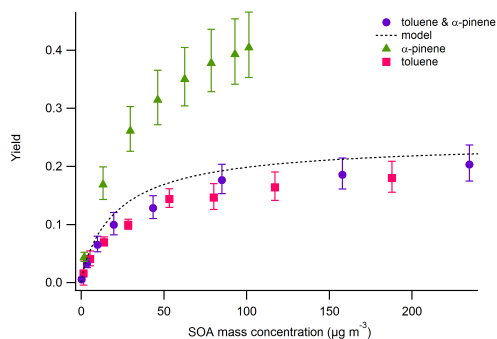


**Figure 27:** Yield diagram for the toluene,  $\alpha$ -pinene mixture. The two-product model seem to be somewhat overestimating experimental yield.

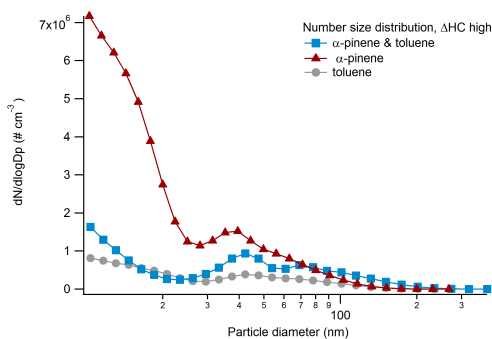


**Figure 28:** Number size distribution at highest  $\Delta HC$  for the [toluene,  $\alpha$ -pinene] mixture experiment as well as individual VOC experiments. Lines between points are present to help guide the eye.

For mass size distribution shown in Figure 29, the mixtures SOA mass was at 150 nm well with in the accumulation mode.

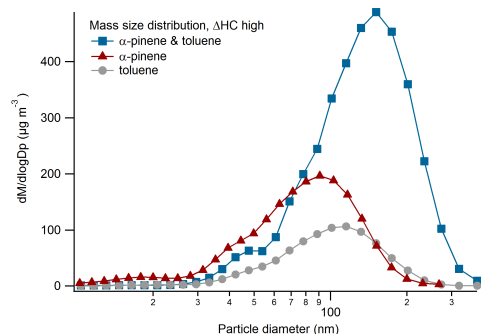


**Figure 29:** Mass size distribution at highest  $\Delta HC$  for the [toluene,  $\alpha$ -pinene] mixture and individual VOCs. Lines between points are present to help guide the eye.

In addition to being shifted to the right, the top was also significantly larger than those from individual VOC experiments. Due to the difference in mixture ratios and  $\Delta HC$ , it is difficult to come to any conclusion regarding SOA formation non-additivity.

## 4.2 Number concentrations in relation to isoprene

It was noted during myrcene mixture experiments that the adding of isoprene affected number concentration to a large degree. This can be seen in Figure 30. The number concentration was reduced approximately by a factor of four for comparable SOA mass concentrations in the [myrcene, m-xylene,  $\alpha$ -pinene, isoprene] experiment compared to previous experiment without isoprene.

Kiendler-Scharr et al. (2009, 2012) likewise observed during experiments that isoprene can inhibit new particle formation and so SOA, although did so in a smog chamber with RH,  $O_3$ -levels different from this study.

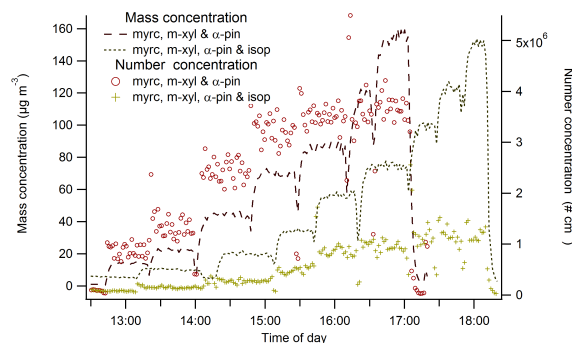


**Figure 30:** Mass and number concentration as a function of time for [myrcene, m-xylene,  $\alpha$ -pinene] and [myrcene, m-xylene,  $\alpha$ -pinene, isoprene] mixtures. Lines between points are present to help guide the eye.

For each of these mixtures' highest SOA mass concentration levels, visible in Figure 30, the isoprene mixture corresponds to  $\Delta HC = 500 \pm 30 \mu g m^{-3}$  and the non-isoprene mixture to  $\Delta HC = 380 \pm 23 \mu g m^{-3}$ . This difference in VOC mass concentration relative to SOA mass concentration is explained by the very low yield of isoprene.

It was also observed that number concentrations for both mixtures started to level out at around  $200 \pm 12 \mu\text{g m}^{-3}$  and  $350 \pm 21 \mu\text{g m}^{-3}$  for non-isoprene, isoprene mixture respectively. Comparing number size distributions for these  $\Delta\text{HC}$ -levels (Figure 31), one can clearly see a much lower number of particles in the nucleation mode for the isoprene mixture, and the Aitken mode top is no longer visible.

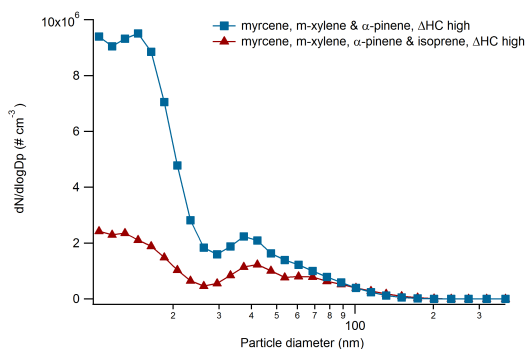


**Figure 31:** Average number size distribution comparing highest  $\Delta\text{HC}$ -levels for the [myrcene, m-xylene,  $\alpha$ -pinene] and [myrcene, m-xylene,  $\alpha$ -pinene, isoprene] mixtures. The effect of isoprene on nucleation mode number concentration is clearly visible, as well as suppressing the visible Aitken mode top. Lines between points are present to help guide the eye.

As for the mass size distribution shown in Figure 32, almost all SOA mass concentration lies between the Aitken mode and accumulation mode, although the non-isoprene mixture have a noticeable mass top in the nucleation mode.

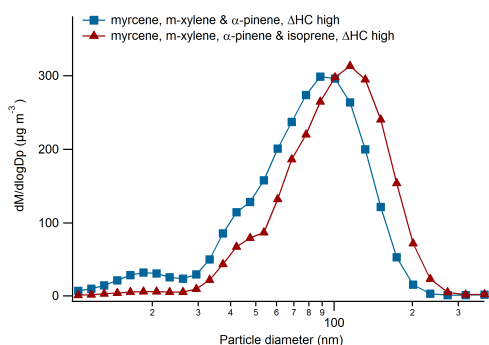


**Figure 32:** Average mass size distribution for the mixtures shown in Figure 31. The non-isoprene mixture has a larger top in the nucleation mode, supported by the much lower number concentration seen in the same region. Lines between points are present to help guide the eye.

The isoprene mixture is not only shifted to the right, but also a bit higher than the non-isoprene mixture. This probably lies within the uncertainty limits. The same effect of much lower number concentration for comparable SOA mass concentrations was noticed in m-xylene experiments with and without isoprene. Also there number concentrations dropped by a factor three to four, even though more measurement points from the isoprene mixture would have been needed to say if this was consistent.

## 5 Set-up evaluation

Several shortcomings were identified during experiments. Most prominent was that air flows fluctuated between 5 - 10 % during experiments, and even more between days. Diffusion chamber pressures fluctuated as well, and although the room in which the experiment was located was exposed to fluctuations in pressure and temperature no correlation between that and the set-up reading fluctuations could be made.

The set-up used a rather crude method of measuring flows which included opening up the piping, briefly exposing the experiment flows to room air and rerouting them through the flow meter.

This caused room air to briefly contaminate the experiment flow and small quantities of VOCs to enter the room, and although this most probably did not affect results nor was dangerous, a more preferred method would have been to have on-line flow meters, negating any need disrupt flows.

The purpose was to use Tenax pipes to analyze and obtain VOC mass concentrations. However, the results from these were unusable. It is unclear where the problem lies, but if this method will be used in the future, extensive testing should be made, preferably in conjunction with longer weighing tests to validate results.

Furthermore since there was a gate valve on the main pipe line, when measuring the  $Q_4$  flow there was a risk of causing pressure build up if forgoing to open up this valve prior to closing the flow meter connection ports. To prevent any damage from this or other unforeseen blockage, a pressure relief valve should be considered upstream along the main line.

The diffusion chamber had an issue with capillaries longer than 7 cm. These would be needed to get highly volatile like toluene down to emission rates more comparable to others like  $\alpha$ -pinene. Their length caused them to be close to the lid and at level with the source of outgoing flow, possibly affecting emission rates. The maximum length that was used in experiments was 7 cm, but it is not wholly dismissible that a higher diffusion chamber would be preferable. The bottom metal cylinder, which held vials in place and distributed incoming purified air to flow upwards past the vials could possibly use some improvement. Mainly more holes for up-flowing air, possibly a series of holes surrounding each vial slot. It was also limited to testing VOC mixtures with four or less components, so for more complex mixtures one would have to modify the cylinder. Although at that point a larger chamber might be needed.

The diffusion chamber and incoming air was also meant to have a stable temperature of 24 °C, to allow for a steady VOC emission. It is not certain that this was fully achieved as no temperature meters were used directly around the chamber flows more than momentarily. It would be a good choice to continuously measure temperature immediately after outgoing flow, for an extended period of time to evaluate if the current set-up is temperature stable.

Another issue was the UV lamp voltage source, which constantly fluctuated  $\pm 3V$ . It is unclear how well the reading fluctuations actually corresponded to voltage output, but it is definitely a possible source for unnecessary inaccuracy.

The set-up does have good potential to become automated. This could for example be achieved by replacing  $Q_1$  and  $Q_3$  needle valves with mass flow controller (MFC), although this would require on-line flow meters that can be connected to the control software. An MFC on  $Q_1$  would make sure that this flow could be stabilized pre-diffusion chamber, increasing certainty in VOC mass concentrations based on emission rates. Such a configuration would probably be preferred even if the set-up also had an on-line method for measuring VOC mass concentrations, such as an PTR-MS. This control software could then be programmed for a timetable of a set

of reacting VOC mass concentrations it should run, forgoing the need for constant supervision. It could even be possible for control software on one machine to parse the current SMPS data file, to calculate the mean slope of volume concentration from present to a desired amount of time backwards, to evaluate if equilibrium have been reached and move on to the next VOC setting. Then, connected to the air humidity system and possibly even a computer controlled UV lamp voltage source, it could be turned in to a quite efficient experiment set-up.

## 6 Conclusion

The purpose of this work was to study the yield of secondary organic aerosol (SOA) mass from the oxidation of a mixture of gas-phase anthropogenic and biogenic volatile organic compounds, using a potential aerosol mass (PAM) chamber with an air of  $RH = 30.6 \pm 0.3\%$ . The purpose was also to evaluate the experiment set-up used.

SOA formation mass concentrations from five individual volatile organic compounds (VOC)  $\alpha$ -pinene, myrcene, m-xylene, isoprene & toluene, as well as from six mixtures of these VOCs were measured for various VOC mass concentrations. Corresponding two-product models were established for each individual VOC, and based on these models an additive approximation of the mixture yields was calculated and compared with experimental results.

For all mixtures experimentally obtained yield, model approximations fell partially or completely within established uncertainty limits. As for experiments involving myrcene, as no emission rate could be experimentally obtained, two cases were tried based on theoretically calculated emission rates.

In no experiments could non-additive yield effects from mixing AVOCs and BVOCs be conclusively observed. However, further experiments might be necessary to confirm this.

The mixture best matching model yield was the mixture of m-xylene & isoprene, and the mixture of toluene and  $\alpha$ -pinene which were both 4 % lower. For all points, except two for the toluene &  $\alpha$ -pinene mixture, were the models covered by experimental uncertainty limits. Worst was the

mixture mixture myrcene, m-xylene which had an experimental yield 30 % higher than model yield for both myrcene cases, and uncertainties covered only the two last model yield points.

Moreover, no non-additive effects could be deduced from looking at particle size distributions for corresponding mixtures.

For the mixtures where  $\Delta HC$  from individual VOCs was comparable to mixture components, mass size distributions showed roughly additive behavior. For some mixtures, mass size distribution tops were shifted relative to individual VOCs mass tops meaning overall bigger particles. The implications for this are unclear as this experiment only looked at SOA particles at the time of formation, and as such how they would change after a period of time is not studied here.

There could be several reasons as to why these experiments didn't show any definitive non-additive effects from aging AVOC and BVOC mixtures, as experiments were performed under comparatively simple conditions. For one, the experiments were performed under  $NO_x$ -free conditions, whereas AVOCs are typically present in an environment containing some level of  $NO_x$ . This due to also potentially forming from human activities such as combustion.  $NO_x$  concentrations does influence SOA yields, and it's effect on VOCs is complex and not fully understood (Hoyle et al., 2011).

Seed particles could also play a role in non-additivity. For example both  $SO_2$  and  $NO_x$ , often created from human activities can for example lead to seed particles in the form of sulphuric and nitric acid. This can also affect SOA yield to a significant extent (Hoyle et al., 2011). Future experiments including these parameters could therefor be of value in further exploring non-additive effects of SOA formation.

The two mixture experiments involving isoprene showed some interesting properties. For comparable amounts of reacted VOC mass, isoprene lowered number concentration, generally by a factor of four, mainly of particles in the nucleation mode. Possibly connected to this observation is that isoprene seemed to elongate the yield curve which can be seen in Figure 23,

i.e. that a higher amount of SOA mass would be required to achieve a corresponding yield of the non-isoprene mixture. It was also observed with direct model approximations for the [myrcene, m-xylene,  $\alpha$ -pinene] mixtures with and without isoprene, that yield for the isoprene-containing mixture would surpass the other at around  $600 \mu g m^{-3}$  SOA mass concentration.

The experiment set-up functioned sufficiently for the purpose of this thesis, but it would be very beneficial to revise and improve parts of its design. As long as an on-line VOC mass concentration measurement device such as a PTR-MS will not be used, then it would be important to have much more supervision over diffusion chamber parameters, such as flow, temperature and pressure, preferably with on-line methods. Tenax pipe measurements proved to be problematic, and need to be revised if it continues to be used.

## Acknowledgments

I would like extend my sincerest thanks to the good people at the Aerosol division of Dept. of Physics, Lund university, who were fundamental in writing this thesis; PhD candidate Erik Ahlberg, who designed the set-up and provided endless essential support to both theory and experimental work; My supervisors Prof. Erik Swietlicki and senior researcher Birgitta Svenningsson, who not only helped me find this topic and provided answers to many questions, but also aided me in administrative matters.

A thanks also goes out to PhD candidate Axel Eriksson who provided a lot of interesting information and support regarding the Aerodyne AMS and data handling, as well as general theory regarding aerosols.

I would also like to thank The Swedish Research Council for Environment, Agricultural Sciences and Spatial Planning (FORMAS) project *Natural organic aerosols under anthropogenic control: formation and implications for climate feedback* (Reg.Nr. 2011-732) for providing funding for these experiments.



## References

- Boucher, O., D. Randall P. Artaxo C. Bretherton G. Feingold P. Forster V.-M. Kerminen Y. Kondo H. Liao U. Lohmann P. Rasch S.K. Satheesh S. Sherwood B. Stevens and X.Y. Zhang (2013), *Climate Change 2013: The Physical Science Basis. Contribution of Working Group I to the Fifth Assessment Report of the Intergovernmental Panel on Climate Change*, Cambridge University Press.
- Canagaratna, M.R., J.T. Jayne, J.L. Jimenez, J.D. Allan, M.R. Alfarra, Q. Zhang, T.B. Onasch, F. Drewnick, H. Coe, A. Middlebrook, A. Delia, L.R. Williams, A.M. Trimborn, M.J. Northway, P.F. DeCarlo, C.E. Kolb, P. Davidovits and D.R. Worsnop (2007), ‘Chemical and microphysical characterization of ambient aerosols with the aerodyne aerosol mass spectrometer’, *Mass Spectrometry Reviews* **26**(2), 185–222.
- Davidson, Cliff I., Robert F. Phalen and Paul A. Solomon (2005), ‘Airborne particulate matter and human health: A review’, *Aerosol Science and Technology* **39**(8), 737–749.
- Dorn, H.-P., R. L. Apodaca, S. M. Ball, T. Brauers, S. S. Brown, J. N. Crowley, W. P. Dubé, H. Fuchs, R. Häsel, U. Heitmann, R. L. Jones, A. Kiendler-Scharr, I. Labazan, J. M. Langridge, J. Meinen, T. F. Mentel, U. Platt, D. Pöhler, F. Rohrer, A. A. Ruth, E. Schlosser, G. Schuster, A. J. L. Shillings, W. R. Simpson, J. Thieser, R. Tillmann, R. Varma, D. S. Venables and A. Wahner (2013), ‘Intercomparison of no<sub>3</sub> radical detection instruments in the atmosphere simulation chamber saphir’, *Atmospheric Measurement Techniques* **6**(5), 1111–1140.
- Emanuelsson, E. U., M. Hallquist, K. Kristensen, M. Glasius, B. Bohn, H. Fuchs, B. Kammer, A. Kiendler-Scharr, S. Nehr, F. Rubach, R. Tillmann, A. Wahner, H.-C. Wu and Th. F. Mentel (2013), ‘Formation of anthropogenic secondary organic aerosol (soa) and its influence on biogenic soa properties’, *Atmospheric Chemistry and Physics* **13**(5), 2837–2855.
- Fuller, Edward N., Paul D. Schettler and J. Calvin. Giddings (1966), ‘New method for prediction of binary gas-phase diffusion coefficients’, *Industrial & Engineering Chemistry* **58**(5), 18–27.
- Fushimi, Akihiro, Rota Wagai, Masao Uchida, Shuichi Hasegawa, Katsuyuki Takahashi, Miyuki Kondo, Motohiro Hirabayashi, Yu Morino, Yasuyuki Shibata, Toshimasa Ohara, Shinji Kobayashi and Kiyoshi Tanabe (2011), ‘Radiocarbon (14c) diurnal variations in fine particles at sites downwind from Tokyo, Japan in summer’, *Environmental Science & Technology* **45**(16), 6784–6792.
- Goldstein, Allen H. and Ian E. Galbally (2007), ‘Known and unexplored organic constituents in the earth’s atmosphere’, *Environmental Science & Technology* **41**(5), 1514–1521.
- Hallquist, M., J. C. Wenger, U. Baltensperger, Y. Rudich, D. Simpson, M. Claeys, J. Dommen, N. M. Donahue, C. George, A. H. Goldstein, J. F. Hamilton, H. Herrmann, T. Hoffmann, Y. Iinuma, M. Jang, M. E. Jenkin, J. L. Jimenez, A. Kiendler-Scharr, W. Maenhaut, G. McFiggans, Th. F. Mentel, A. Monod, A. S. H. Prévôt, J. H. Seinfeld, J. D. Surratt, R. Szmigielski and J. Wildt (2009), ‘The formation, properties and impact of secondary organic aerosol: current and emerging issues’, *Atmospheric Chemistry and Physics* **9**(14), 5155–5236.
- Heald, C. L., H. Coe, J. L. Jimenez, R. J. Weber, R. Bahreini, A. M. Middlebrook, L. M. Russell, M. Jolleys, T.-M. Fu, J. D. Allan, K. N. Bower, G. Capes, J. Crosier, W. T. Morgan, N. H. Robinson, P. I. Williams, M. J. Cubison, P. F. DeCarlo and E. J. Dunlea (2011), ‘Exploring the vertical profile of atmospheric organic aerosol: comparing 17 aircraft field campaigns with a global model’, *Atmospheric Chemistry and Physics* **11**(24), 12673–12696.
- Hoyle, C. R., M. Boy, N. M. Donahue, J. L. Fry, M. Glasius, A. Guenther, A. G. Hallar, K. Huff Hartz, M. D. Petters, T. Petäjä, T. Rosenoern and A. P. Sullivan (2011), ‘A review of the anthropogenic influence on biogenic secondary organic aerosol’, *Atmospheric Chemistry and Physics* **11**(1), 321–343.
- Kanakidou, M., J. H. Seinfeld, S. N. Pandis, I. Barnes, F. J. Dentener, M. C. Facchini, R. Van Dingenen, B. Ervens, A. Nenes, C. J. Nielsen, E. Swietlicki, J. P. Putaud, Y. Balkanski, S. Fuzzi, J. Horth, G. K. Moortgat, R. Winterhalter, C. E. L. Myhre, K. Tsigaridis, E. Vignati, E. G. Stephanou and J. Wilson (2005), ‘Organic aerosol and global climate modelling: a review’, *Atmospheric Chemistry and Physics* **5**(4), 1053–1123.
- Kang, E., D. W. Toohey and W. H. Brune (2011), ‘Dependence of soa oxidation on organic aerosol mass concentration and OH exposure: experimental chamber studies’, *Atmospheric Chemistry and Physics* **11**(4), 1837–1852.
- Kang, E., M. J. Root, D. W. Toohey and W. H. Brune (2007), ‘Introducing the concept of potential aerosol



- mass (pam)', *Atmospheric Chemistry and Physics* **7**(22), 5727–5744.
- Kiendler-Scharr, A., S. Andres, M. Bachner, K. Behnke, S. Broch, A. Hofzumahaus, F. Holland, E. Kleist, T. F. Mentel, F. Rubach, M. Springer, B. Steitz, R. Tillmann, A. Wahner, J.-P. Schnitzler and J. Wildt (2012), 'Isoprene in poplar emissions: effects on new particle formation and oh concentrations', *Atmospheric Chemistry and Physics* **12**(2), 1021–1030.
- Kiendler-Scharr, Astrid, Jürgen Wildt, Miikka DalMaso, Thorsten Hohaus, Einhard Kleist, Thomas F. Mentel, Ralf Tillmann, Ricarda Uerlings, Uli Schurr and Andreas Wahner (2009), 'New particle formation in forests inhibited by isoprene emissions', *Nature* **461**(7262), 381–384.
- Kuwata, Mikinori, Soeren R. Zorn and Scot T. Martin (2012), 'Using elemental ratios to predict the density of organic material composed of carbon, hydrogen, and oxygen', *Environmental Science & Technology* **46**(2), 787–794.
- Lambe, A. T., A. T. Ahern, L. R. Williams, J. G. Slowik, J. P. S. Wong, J. P. D. Abbatt, W. H. Brune, N. L. Ng, J. P. Wright, D. R. Croasdale, D. R. Worsnop, P. Davidovits and T. B. Onasch (2011), 'Characterization of aerosol photooxidation flow reactors: heterogeneous oxidation, secondary organic aerosol formation and cloud condensation nuclei activity measurements', *Atmospheric Measurement Techniques* **4**(3), 445–461.
- Lyman, W.J., Reehl W.F. Rosenblatt D.H. (1990), *Handbook of chemical property estimation methods: Environmental behavior of organic compounds*, American Chemical Society, Washington, DC.
- McKelvey, J. M. and H. E. Hoelscher (1957), 'Apparatus for preparation of very dilute gas mixtures', *Analytical Chemistry* **29**(1), 123–123.
- Nakao, Shunsuke, Ping Tang, Xiaochen Tang, Christopher H. Clark, Li Qi, Eric Seo, Akua Asa-Awuku and David Cocker III (2013), 'Density and elemental ratios of secondary organic aerosol: Application of a density prediction method', *Atmospheric Environment* **68**(0), 273 – 277.
- Ng, N. L., J. H. Kroll, A. W. H. Chan, P. S. Chhabra, R. C. Flagan and J. H. Seinfeld (2007), 'Secondary organic aerosol formation from m-xylene, toluene, and benzene', *Atmospheric Chemistry and Physics* **7**(14), 3909–3922.
- Odum, Jay R., Thorsten Hoffmann, Frank Bowman, Don Collins, Richard C. Flagan and John H. Seinfeld (1996), 'Gas/particle partitioning and secondary organic aerosol yields', *Environmental Science & Technology* **30**(8), 2580–2585.
- Pankow, James F. (1994a), 'An absorption model of gas/particle partitioning of organic compounds in the atmosphere', *Atmospheric Environment* **28**(2), 185 – 188.
- Pankow, James F. (1994b), 'An absorption model of the gas/aerosol partitioning involved in the formation of secondary organic aerosol', *Atmospheric Environment* **28**(2), 189 – 193.
- Pope, C. Arden and Douglas W. Dockery (2006), 'Health effects of fine particulate air pollution: Lines that connect', *Journal of the Air & Waste Management Association* **56**(6), 709–742.
- Roldin, P., Zhou J. Swietlicki E. Massling A. (2008), *Lund SMPS User's Manual*, Lund University, Lund, Sweden.
- Setyan, A., Q. Zhang, M. Merkel, W. B. Knighton, Y. Sun, C. Song, J. E. Shilling, T. B. Onasch, S. C. Herndon, D. R. Worsnop, J. D. Fast, R. A. Zaveri, L. K. Berg, A. Wiedensohler, B. A. Flowers, M. K. Dubey and R. Subramanian (2012), 'Characterization of submicron particles influenced by mixed biogenic and anthropogenic emissions using high-resolution aerosol mass spectrometry: results from cares', *Atmospheric Chemistry and Physics* **12**(17), 8131–8156.
- Shen, Xiaoli, Yue Zhao, Zhongming Chen and Dao Huang (2013), 'Heterogeneous reactions of volatile organic compounds in the atmosphere', *Atmospheric Environment* **68**(0), 297 – 314.
- Shilling, J. E., Q. Chen, S. M. King, T. Rosenorn, J. H. Kroll, D. R. Worsnop, K. A. McKinney and S. T. Martin (2008), 'Particle mass yield in secondary organic aerosol formed by the dark ozonolysis of  $\alpha$ -pinene', *Atmospheric Chemistry and Physics* **8**(7), 2073–2088.
- Spracklen, D. V., J. L. Jimenez, K. S. Carslaw, D. R. Worsnop, M. J. Evans, G. W. Mann, Q. Zhang, M. R. Canagaratna, J. Allan, H. Coe, G. McFiggans, A. Rap and P. Forster (2011), 'Aerosol mass spectrometer constraint on the global secondary organic aerosol budget', *Atmospheric Chemistry and Physics* **11**(23), 12109–12136.

Thermodynamics Research Center, NIST Boulder Laboratories, M. Frenkel director (2011), *NIST Chemistry WebBook, NIST Standard Reference Database 69*, National Institute of Standards and Technology. (retrieved May 18, 2014).

**URL:** <http://webbook.nist.gov>

Thomson, George Wm. (1946), 'The antoine equation for vapor-pressure data.', *Chemical Reviews* **38**(1), 1-39.

**URL:** <http://dx.doi.org/10.1021/cr60119a001>

Volkamer, Rainer, Jose L. Jimenez, Federico San Martini, Katja Dzepina, Qi Zhang, Dara Salcedo, Luisa T. Molina, Douglas R. Worsnop and Mario J. Molina (2006), 'Secondary organic aerosol formation from anthropogenic air pollution: Rapid and higher than expected', *Geophysical Research Letters* **33**(17), n/a-n/a.

Wilke, C. R. and C. Y. Lee (1955), 'Estimation of diffusion coefficients for gases and vapors', *Industrial & Engineering Chemistry* **47**(6), 1253-1257.

## Appendix A: MATLAB code

### SMPSeval code

This code loads Lund SMPS \*.inv files and allows the user to select intervals from the time series, from which a number of values are calculated and made available to the user.

The code makes use of a third-party script named `dynamicDateTicks.m`, which enables dynamic time ticks when zooming on the x-axis.

---

```

function evalSMPS9
% Program for evaluating Lund SMPS inverted (*.inv) data files.
% Press "Process new interval, choose left and right interval by clicking
% on volume vs time plot. To save a series of measurements with a custom tag
% enter desired tag in the process tag textbox and press "process new interval and save"
% Will create arrays in workspace containing
% - mean, rms and std values for volume and number concentration, samples size
% - Mean nbr and volume size distribution, corresponding particle diameter
% - Array containing strings of start and end time of interval

%import data from dir
delimiter = '\t';
% startRow = 1;

filedir = uigetdir('fileroot','Select_folder_with_SMPS_*.inv-files');
cd(filedir);

filearray = dir([filedir '/*.inv']); %Inventory all inv-files in directory
namearray = repmat({''},length(filearray),1); %Pre-allocate cell array
namestring = '';

for ip = 1:length(filearray) %Create one cell array with strings of file names in dir, and one string for
    popupmenu
    namearray(ip) = {filearray(ip).name};
    namestring = [namestring '|' filearray(ip).name];
end

uicontrol('Style','popup',... %popupmenu with file names
    'String',namestring,...
    'Units','normalized',...
    'Position',[0.01 0.9 0.07 0.04],...
    'Callback',@loadinv);
uicontrol('style','text',... %describing text for popup
    'Units','normalized',...
    'Position',[0.01 0.95 0.07 0.03],...
    'String','Open_file_from_current_dir');
uicontrol('Style','pushbutton',... %Optionally, open individual inf-file specifically
    'String','Open_other_file',...
    'Units','normalized',...
    'Position',[0.01 0.7 0.07 0.04],...
    'Callback',@loadspecfile);

%Function for loading a specific file
function loadspecfile(hObj,event) %#ok<INUSD>
    [filename1,filepath1]=uigetfile({'*.inv','inv-Files'},...
    'Select_Data_File');
    cd(filepath1);
    fp = fopen(filename1, 'r'); %create handle for file to analyze
    evalfile(filename1);
    set(hMain,'name',filename1);
    updateMainPlot;
end

%Function for loading chosen file in popup menu
function loadinv(hObj,event) %#ok<INUSD>
    val = get(hObj,'Value') - 1; %compensate for empty space in first popup slot
    filename1 = namearray{val};
    fp = fopen(filename1, 'r'); %create handle for file to analyze
    evalfile(filename1);
    xcoord = [0, size(data(:,5))];
    ginputon = false;
    set(hMain,'name',filename1);
    updateMainPlot;
    tagAsDate;
    newFileLog;
end

%Variables that needs to be global
formatSpec = '%[\n\r]';
printlog = '\r\n\r\n';
ncols = 0;
timecent = 0;
time = 0;
dataraw = 0;
data = 0;
% dplot = 0;
filename1 = namearray{1};
fp = fopen(filename1, 'r'); %create handle for file to analyze
evalfile(filename1);
ginputon = false;

function evalfile(filename1) %extract data from loaded file, arrange into matrices
%evaluate number of columns the file has, and write formatSpec accordingly
    fp2 = fopen(filename1, 'r'); %open same file again

```

```

prevncols = 0; %previous max number of columns
while 1
    tline = fgetl(fp2); %read next line in file
    if isnumeric(tline), break, end %breaks loop if next line doesn't contain a number
    ncols = sum(tline == '-----') + 1; %count nbr. columns
    if ncols > prevncols
        prevncols = ncols;
    end
end
for i = 1:ncols
    formatSpec = ['%f', formatSpec]; %write a new formatSpec based on number of columns
    printlog = ['%f\t', printlog]; %write a formatspec for printing out sizedistribution info to log
end

fgets(fp);
A = textscan(fp, formatSpec, 'Delimiter', delimiter, 'EmptyValue', .NaN, 'ReturnOnError', false);
fclose(fp);
data = [A{1:end-1}]; %creates a double-values matrix from imported text
dataraw = data; %keep a matrix of the raw data

data = data(:,1:5);

%Remove duplicate rows in data file
r = max(size(data)); % total rows
d = 2; % rows in each data set
n = 1; % remove first n rows in each data set
data(mod(2:r,d)<=n & mod(2:r,d)>0,:) = [];

timecent = data(:,1); %creates a vector with the time values
time = cellstr(datestr(timecent, 'HH:MM:SS')); %converts to string with time in hours:min:sec

end
%% Main graphical components
hMain = figure(1);
% subplot(2,1,1)
subplot(2,8,1:6)
hMainpos = [0.01 0.3 0.98 0.5];
set(hMain, 'Units', 'normalized', 'Position', hMainpos); %old fig sizepos: [10 400 1900 500]
set(gcf, 'name', filename1);
mTitleBox = uicontrol('style','text','Position',[30 45 130 50],'String','Mean_μm^3/cm^3:-(
    Automatically_copies_to_clipboard)'); %create text box for title
mTextBox = uicontrol('style','edit','Position',[30 30 130 20]); %create text box for outputting
    calculated mean value
set(mTextBox,'String','...');
mTimeBox = uicontrol('style','edit','Position',[30 5 130 20]); %create text box for outputting
    calculated mean value
set(mTimeBox,'String','...');
set(gcf, 'toolbar', 'figure'); %force toolbar to be visible

%Create two y-axes (one for vol, one for nbr)
ax1 = gca;
set(gca, 'xcolor',[1 1 1]) %makes a second, redundant x-axis near invisible
%Set(gca, 'xcolor', get(gcf, 'color'))
set(gca, 'XTick', []);
set(ax1, 'YAxisLocation', 'right');
ylabel('Number_concentration_-(#/cm^3)');
hold on
hNbr = plot(timecent, data(:,3), 'r-'); %NBRconcddata plot
ax2 = axes('Position',get(ax1,'Position'),...
    'YAxisLocation','bottom',...
    'YAxisLocation','left',...
    'Color','none',...
    'XColor','k','YColor','k');
linkaxes([ax1 ax2], 'x');
hold on
hVol = plot([0 1], [min(data(:,5)) max(data(:,5))], 'b-', 'Parent', ax2); %VOLconcddata plot
xlabel('Time_of_Day');
ylabel('Volume_concentration_-(μm^3/cm^3)');
title('SMPS_data');
grid on

dynamicDateTicks([], [], ''); %3rd party software. Modifies x-axis to dynamically show time.

newFileLog;

%choice of interval for mean calc.
xcoord = [0 0];
h1 = plot([xcoord(1) xcoord(1)], [0 max(data(:,3))], 'k-');
h2 = plot([xcoord(2) xcoord(2)], [0 max(data(:,3))], 'k-');

%Size distribution plot
subplot(2,8,9:11)
h3 = semilogx(0,0);
title('Size_distribution');
xlabel('Dp_(nm)');
ylabel('dV/dlogDp');
hold on

%Nbr distribution plot
subplot(2,8,12:14)
h4 = semilogx(0,0);
title('Number_distribution');
xlabel('Dp_(nm)');
ylabel('dN/dlogDp_(cm)');
hold on

%Create empty arrays for table
voidatatable = zeros(1,6);
distdatatable = zeros(ncols,3);

```

```

%Create data tables for fetching data live
ssizetemp = get(0,'ScreenSize');
ssize = ssizetemp(3);
tablepos = [0.74 0.001 0.25 0.89];
datatable = uitable('Data', [1 2 3],...
    'ColumnName', {'Nothing', 'to', 'show', 'yet', '...'},...
    'Units', 'normalized',...
    'Position', tablepos,... %old pix [1390 1 500 450]
    'ColumnWidth', {tablepos(3)*hMainpos(3)*ssize*1/7-5});

%process name tag for saving to workspace
procnameold = filename(1:end-4);
procnum = 1;
processref = uicontrol('style','edit',... %Process tag window, for naming
    'Units', 'normalized',...
    'Position', [0.62 0.926 0.07 0.035],...
    'String', procnameold);
tablewarning = uicontrol('style','text',... %Text
    'Units', 'normalized',...
    'Position', [0.605 0.9636 0.10 0.03],...
    'String', 'Process_tag_for_saving_to_workspace:');
tablewarning = uicontrol('style','text',... %text
    'Units', 'normalized',...
    'Position', [0.74 0.89 0.26 0.026],...
    'String', 'WARNING:_MATLAB_table_unreliable_for_copypasting_values._Use_created_
workspace_matrices_instead. ');
timetabletitle = uicontrol('style','text',... %text
    'Units', 'normalized',...
    'Position', [0.868 0.9636 0.1 0.026],...
    'String', 'Time_interval');
timetable = uicontrol('style','edit',... %Textbox showin timeinterval processed
    'Units', 'normalized',...
    'Position', [0.868 0.9176 0.1 0.04]);

%Buttons for starting evaluating interval
evalbtn = uicontrol('Style', 'pushbutton',... %will not save previous sessions, only send current to
workspace
    'String', 'Process_new_interval',...
    'Units', 'normalized',...
    'Position', [0.45 0.93 0.06 0.06],...
    'Callback', @evalintervalnosave);
evalbtnsave = uicontrol('Style', 'pushbutton',... %will save previous to workspace, with associated
tag from editbox
    'String', 'Process_new_interval_and_save',...
    'Units', 'normalized',...
    'Position', [0.52 0.93 0.08 0.06],...
    'Callback', @evalintervalsave);

%btngroup for selecting what data one desires shown
h = uibuttongroup('visible','on','Units','normalized','Position',[0.73 0.93 0.12 0.06]);

u0 = uicontrol('Style','pushbutton',... %Volume data to datatable
    'String','Get_vol_conc_data',...
    'Units','normalized',...
    'pos',[0 0 0.5 1],...
    'parent',h,...
    'HandleVisibility','off',...
    'Callback', @voldata);
u1 = uicontrol('Style','pushbutton',... %Nbr. data to datatable
    'String','Get_size_dist_data',...
    'Units','normalized',...
    'pos',[0.5 0 0.5 1],...
    'parent',h,...
    'HandleVisibility','off',...
    'Callback', @distdata);

%Update functions for data table
function voldata(hObject,event) %%ok<INUSD>
    % Called when user activates popup menu
    set(datatable,'ColumnName',{'Vol_mean','Nbr_mean','Vol_std','Nbr_std','Vol_rms','Nbr_rms',
samples});
    set(datatable,'Data',[voldatatable]);
end

function distdata(hObject,event) %%ok<INUSD>
    % Called when user activates popup menu
    set(datatable,'ColumnName',{'Vol_dist','Nbr_dist','Dp'});
    set(datatable,'Data',[distdatatable]);
end

%Pre-allocate name and gather arrays
volcolname = [{'vol_mean'},{'nbr_mean'},{'vol_std'},{'nbr_std'},{'vol_rms'},{'nbr_rms'},{'samples'}];
distcolname = [{'vol_size_dist'},{'nbr_size_dist'},{'Dp'}];

%Gather arrays
procvol = [{'tag'}, volcolname];
procdist = repmat({''},0,3);
proctime = [{'tag'},{'From'},{'To'}];

%Functions to start processing, with and without saving
savetoworkspace = true;
function evalintervalnosave(~,~)
    savetoworkspace = false;
    ginputon = true;
    evalinterval;
end

function evalintervalsave(~,~)

```

```

savetoworkspace = true;
ginputon = true;
evalinterval;
end
function evalinterval(hObject,event) %#ok<INUSD>

if ginputon
[xcoord, ~] = ginput(2); %Get mouse coordinates
end
[~,idx(1)] = min(abs(timecent - xcoord(1))); %Find corresponding index for mouse coordinates
[~,idx(2)] = min(abs(timecent - xcoord(2))); %-|-
assignin('base','timecent',timecent);
row = idx(1)*2;
idx = sort(idx);
yintnbr = data(idx(1):idx(2),3); %y-vals for chosen interval, #/cm3
yintvol = data(idx(1):idx(2),5); %y-vals for chosen interval, vol/cm3
xint = timecent(idx(1):idx(2)); %x-vals for interval
nbr_rms_mean = [rms(yintnbr), mean(yintnbr)'] %rms & mean for #-conc
vol_rms_mean = [rms(yintvol), mean(yintvol)'] %rms & mean for vol-conc
std_nbrconc = std(yintnbr) %standarddeviation for #-conc
std_volconc = std(yintvol) %std-deviation for vol-conc
from_time = time(idx(1)) %time at beginning of chosen interval
nbr_samples = idx(2) - idx(1); %how many samples data is based on

%Calcualte mean size dist in given interval
tx = floor(idx(1)/2)*4; %Round down to nearest even to fit with corresponding SMPS data row
ty = floor(idx(2)/2)*4;
assignin('base','idx',idx);
assignin('base','nbrdistslotx',tx+1:2:ty);
assignin('base','tx',tx);
assignin('base','ty',ty);

nbrdist = dataraw(tx+1:2:ty,6,ncols);
assignin('base','asdasdasd111a',nbrdist);
assignin('base','asdasdas22222a',dataraw);
dr = dataraw(tx:2:ty-1,6,ncols)*1E-3; %diameter for each data point, um
Vp = (1/6)*pi*(dr).^3; % volume for each data point, um3
sizedist = nbrdist.*Vp;
dplot = dataraw(tx,6,ncols); %x values for diameter, nm
meanmassdist = mean(sizedist,1); %Calc. mean mass size dist from interval
meannbrdist = mean(nbrdist,1); %Calc. mean nbr size dist from interval

%Create arrays with relevant size dist data, for display in datatable
voldatatable = [vol_rms_mean(2), nbr_rms_mean(2), std_volconc, std_nbrconc, vol_rms_mean(1),
    nbr_rms_mean(1), nbr_samples];
distdatatable = [meanmassdist, meannbrdist, dplot'];
timeinterval = [time{idx(1)}, '- ', time{idx(2)}];
set(timetable,'String',timeinterval); %updates textbox with current selected time interval

%Creates name array for data, send to workspace
volnamedtable = [volcolname;num2cell(voldatatable)];
distnamedtable = [distcolname;num2cell(distdatatable)];
assignin('base','lastvolnbrdata',volnamedtable); %Sends array to workspace
assignin('base','lastsizedistdata',distnamedtable); %Sends array to workspace
assignin('base','lasttimeinterval',timeinterval); %array with times between interval

%create accumulating array with tagged values for each process
if savetoworkspace
    procname = get(processref,'String'); %Get string from namebox
    if strcmpi(procname,'Not_saved')
        procname = 'Very_saved';
    end

    if strcmpi(procname,procnameold) && ~isempty(procvol) %compare old string with new, if equal and
        not first process, proceed
        ind = find(procname == '-'); %find dash
        if ~isempty(ind)
            procname = procname(1:ind(end)-1); %remove dash for comparison
        end
        procname = [procname '-' num2str(procnum)]; %add current nbr of processes with this name
        procnum = procnum + 1; %add nbr of processes done with this name
    elseif ~isempty(procvol) %If name differs from previous, and not first time, proceed
        prevnames = procvol(:,1); %make an array of the previous names
        exist = false;
        prevnum = 0;
        for ik = 2:length(prevnames) %look through all previos names excluding dash and number
            ind = find(prevnames{ik} == '-');

            if strcmpi(procname,prevnames{ik}(1:ind(end)-1)) %if found, set condition true and add
                current
                exist = true; %number for found name
                currnum = str2num(prevnames{ik}(ind(end)+1:end));
                if currnum > prevnum
                    prevnum = currnum; %change highest number found
                end
            end
            procnum = prevnum + 1; %add to highest number
        end
        if exist %if name used previously, add "-1", increase counter
            procname = [procname '-' num2str(procnum)];
            procnum = procnum + 1;
        else %if not, add "-1" to name and increase counter
            procname = [procname '-' num2str(1)];
            procnum = procnum + 1;
        end
    else %first time, (procvol empty) always add "-1" to name and increase counter
        procname = [procname '-' num2str(1)];
        procnum = procnum + 1;
    end
    procvol = [procvol; [{procname}'],volnamedtable(2,:)];
end

```

```

    procdist = [procdist; [{'tag'}, {procname}, {''}]; distnamedtable(:, 1:3) [{''}, {''}, {''}];
    proctime = [proctime; {procname}, time(idx(1)), time(idx(2))];

%send accumulated arrays to workspace
assignin ('base', 'savedvoldata', procvol);
assignin ('base', 'saveddistdata', procdist);
assignin ('base', 'savedtimedata', proctime);

    procnameold = procname; %set prev name for next iteration
    set (processref, 'String', procname); %update name in editbox
end
else
    set (processref, 'String', 'Not_saved');
end

%Reset selection coordinates, thicken lines

set(h1, ... %Updates first interval selection marker
'XData', [xcoord(1) xcoord(1)], ...
'YData', [min(data(:,5)) max(data(:,5))], ...
'LineWidth', 2)
set(h2, ... %Updates second interval selection marker
'XData', [xcoord(2) xcoord(2)], ...
'YData', [min(data(:,5)) max(data(:,5))], ...
'LineWidth', 2)

set(h3, ... %Updates mass size dist plot
'XData', dplot, ...
'YData', meanmassdist, ...
'LineWidth', 2) ;

set(h4, ... %updates nbr size dist plot
'XData', dplot, ...
'YData', meannbrdist, ...
'LineWidth', 2) ;

set(mTextBox, 'String', num2str(mean(yintvol))); %updates calculated volconc mean
set(mTimeBox, 'String', time{idx(1)});
clipboard('copy', num2str(mean(yintvol))); %copies volconc mean to clipboard

fid = fopen('SMPSeval-log.txt', 'at');
fprintf(fid, '\r\n-----\r\n');
fprintf(fid, 'From_%s_%s_%s_%s_%s_%s_%s_%s\r\n', [time{idx(1)} '_(index_x:_' num2str(idx(1)) ')-to_
-----' time{idx(2)} '_(index_y:_' num2str(idx(2)) ')-_Nbr_of_data_points:_' num2str(abs(idx(1)-idx(2))
]);
fprintf(fid, '\r\n\r\n');
fprintf(fid, '%s\t%s\t%s\t%s\t%s\t%s\t%s\t%s\r\n', ['vol_mean_' 'nbr_mean_' 'vol_std_'
'nbr_std_' 'vol_rms_' 'nbr_rms_' 'samples_']);
fprintf(fid, '\r\n');
fprintf(fid, '%f\t%f\t%f\t%f\t%f\t%f\t%f\t%f\r\n', [mean(yintvol) mean(yintnbr) std(yintvol) std(yintnbr)
rms(yintvol) rms(yintnbr) nbr_samples]);
fprintf(fid, '\r\n\r\n');
fprintf(fid, 'Mass-Size-distribution_dMdlogDp-\r\n');
fprintf(fid, printlog, meanmassdist);
fprintf(fid, '\r\n\r\n');
fprintf(fid, 'Number-Size-distribution_dNdlogDp-\r\n');
fprintf(fid, printlog, meannbrdist);
fprintf(fid, '\r\n\r\n');
fprintf(fid, 'Corresponding_particle_diameter_(nm)-\r\n');
fprintf(fid, printlog, dplot);
fclose(fid);

end
function updateMainPlot()
    get(hMain, 'YLim')
    set(hNbr, ... %Updates number conc
'XData', timecent, ...
'YData', data(:,3), ...
'LineWidth', 1);
set(hVol, ... %Updates vol conc
'XData', timecent, ...
'YData', data(:,5), ...
'LineWidth', 1);
xlim(ax2, [min(timecent) max(timecent)]);
ylim(ax2, [min(data(:,5)) max(data(:,5))]);
refresh(hMain)

end
function tagAsDate()
    set(processref, 'String', filename1(1:end-4));
end
function newFileLog()
    %create log of what file has been opened and when, create title column
    fid = fopen('SMPSeval-log.txt', 'at');
    fprintf(fid, '%s', '-----');
    fprintf(fid, '\r\n');
    fprintf(fid, '%s_%s_%s\r\n\r\n', [filename1 ']' datestr(now));
    fprintf(fid, '\r\n\r\n');
    fclose(fid);
end
end
end

```

## Appendix B: Experiment data



$\alpha$ -pinene

Start	Q1 (l/min)	Q4 (l/min)	Q2 (l/min)	C VOC (ug/m <sup>3</sup> )	Vol (um <sup>3</sup> /cm <sup>3</sup> )	Yield	Yield model	O3 (ppb)	std vol	datapoints
09:16	1.56	0.201	6.03	28.8747598091	1.2581	39.0011	0.0435058864	6257	0.044527	27
10:30	1.56	0.4	6.03	55.6838291808	9.3992	151.09214	0.1692319307	5805	0.257595	29
11:33	1.56	0.6	6.03	81.0061134915	21.1596	233.81358	0.2601384021	5835	0.324331	27
12:31	1.56	0.801	6.03	104.9610834166	33.0218	281.6128786517	0.3149839564	5886	0.590308	22
13:17	1.56	1.003	6.03	127.6557524162	44.7109	313.5112260219	0.3513128983	5906	0.669524	23
14:04	1.56	1.2	6.03	148.5672288931	56.1416	338.25314	0.3770259005	5966	0.814024	21
15:00	1.56	1.402	6.03	168.858289383	66.4076	352.0265928673	0.3947978556	5917	1.057637	18
15:34	1.56	1.506	6.03	178.8809761738	72.3996	362.2864446215	0.4034886998	5899	0.989467	29

m-xylene

Start	Q1 (l/min)	Q4 (l/min)	Q2 (l/min)	C VOC (ug/m <sup>3</sup> )	Vol (um <sup>3</sup> /cm <sup>3</sup> )	Yield	Yield model	O3 (ppb)	std vol	datapoints
09:25	1.532	0.2	5.999	46.9031486726	0.01715	0.531566425	0.0002205705	6115	0.004588	39
10:57	1.532	0.4	5.999	90.874392443	1.4128	22.601268	0.015822982	5641	0.074309	18
11:51	1.532	0.6	5.999	132.180308511	7.0116	77.115914	0.0536011561	5853	0.248401	20
13:17	1.532	0.8	5.999	171.0561074402	13.7115	116.530610625	0.0793593314	5578	0.673207	47
14:54	1.532	1.1	5.999	225.2626288798	23.591	152.2477354545	0.1052374872	5658	1.228088	23
15:33	1.532	1.502	5.999	291.1014752495	40.4603	202.0590614514	0.1375551547	5594	1.109808	9

$\alpha$ -pinene, m-Xylene

Start	Q1 (l/min)	Q4 (l/min)	Q2 (l/min)	C aptin (ug/m <sup>3</sup> )	C xyl (ug/m <sup>3</sup> )	Vol (um <sup>3</sup> /cm <sup>3</sup> )	Yield	Yield Model	O3 (ppb)	std vol	data-points
10:15	1.42	0.101	5.91	16.5230787946	26.3535245152	0.30317	0.007070756	0.0072938885	6125	0.024558	29
11:01	1.42	0.2	5.91	32.1888242403	51.3396431304	5.0054	0.0599244803	0.0707135828	5551	0.186853	19
11:48	1.42	0.3	5.91	47.5057285285	75.7693766973	16.9503	0.1374997812	0.1445783988	5518	0.502995	18
12:32	1.42	0.15	5.91	24.340806449	38.8224281593	1.7448	0.0276236645	0.0331560761	5438	0.098897	26
13:21	1.42	0.4	5.91	62.3371524906	99.424792243	28.8205	0.178166132	0.1864191204	5491	1.064282	19
14:08	1.42	0.6	5.91	90.6330488977	144.5545007036	51.9193	0.2207561642	0.2375516393	5433	1.263512	26
15:03	1.42	0.8	5.91	117.242155653	186.9956599265	74.8639	0.2460703311	0.2711156743	5470	1.318991	14
15:35	1.42	1.105	5.91	154.8998263003	247.0578528703	106.8634	0.2658573416	0.3046704487	5597	1.969007	7

isoprene

Start	Qisop (l/min)	Q2 (l/min)	C VOC (ug/m <sup>3</sup> )	Vol (um <sup>3</sup> /cm <sup>3</sup> )	Yield	Yield model	O3 (ppb)	std vol	data-Points
10:30	0.1	6.06	45.1491249037	0.0005	1.10744117647059E-005	1.55256269638879E-006		0.000577	3
10:40	0.2	6.06	88.855785753	0.0005	0.000056271	1.54911866024858E-005	5480	0	0
10:48	0.7	6.06	287.992642877	0.077333	0.0002685242	0.0002315448		0.002828	17
11:20	0.803	6.06	325.4105250674	0.14529	0.0004464822	0.0004222735		0.004256	20
12:02	0.904	6.06	361.0270288683	0.3193	0.0008675888	0.0008675888	5270	0.010883	19
12:40	1.005	6.06	395.6251980948	0.57792	0.0014607765	0.0014466194		0.026665	23
13:36	1.146	6.06	442.3035336947	0.89481	0.0020230677	0.0020680348	4960	0.036156	15
14:18	1.36	6.06	509.7591762715	1.882	0.0036919394	0.0036825276		0.078378	23



myrcene r = 0.9, m-xylene

C myrc (ug/m <sup>3</sup> )	C xyl (ug/m <sup>3</sup> )	Yield	Y sum
10.2255297392	25.3043806015	0.0091995729	0.0063789374
18.851541795	46.6505593259	0.0766201386	0.0539998854
31.4835420936	77.9100513437	0.1381049789	0.1025445032
37.4191937359	92.5989787284	0.1606034283	0.1202552405
56.4263322884	139.6341729555	0.2105446987	0.1625665325
76.8802566724	190.2500237333	0.2169042757	0.1865902970
96.3487408694	238.427276787	0.2366125284	0.2105450473

myrcene r = 0.3, m-xylene,  $\alpha$ -pinene

Start	Q1 (l/min)	Q4 (l/min)	Q2 (l/min)	C myrc (ug/m <sup>3</sup> )	C xyl (ug/m <sup>3</sup> )	C pin (ug/m <sup>3</sup> )	Vol (um3/cm <sup>3</sup> )	Yield	Yield model	O3 (ppb)	std vol	Points
10:22	1.45	0.048	5.98	1.6474841544	12.2307304779	7.6683983307	0.076833	0.0035658969	0.0025729747	4528	0.021833	11
11:18	1.45	0.09	5.98	3.0676589218	22.7739425413	14.2787598242	2.7116	0.0675866297	0.0554400404	5242	0.15202	12
12:05	1.45	0.073	5.98	2.4952004421	18.524077463	11.6141881266	0.6722	0.0205984862	0.0188479842	5201	0.127504	14
12:40	1.45	0.16	5.98	5.3914410873	40.0254306843	25.0950625069	10.0569	0.1426269199	0.1283244619	5200	0.375752	14
13:17	1.45	0.2	5.98	6.6956812856	49.70795801	31.1657936473	15.9576	0.18222797	0.1646008664	5240	0.48171	15
13:57	1.45	0.277	5.98	9.1592939101	67.9982939101	42.6334309677	31.8354	0.265757592	0.2264546178	5281	1.148864	13
14:45	1.45	0.426	5.98	13.758652987	102.1426372884	64.0411814075	49.8825	0.277213598	0.2693425276	5254	1.097442	13
15:26	1.45	0.502	5.98	16.0231516454	118.9540115798	74.5815424094	61.8496	0.2951421169	0.2901772405	5252	1.595598	18
16:09	1.45	0.624	5.98	19.5492804779	145.1315813396	90.9943014521	86.1297	0.3368715948	0.3223781547	5376	1.307767	5
16:31	1.45	0.826	5.98	25.1096902328	186.4114157322	116.8758474254	111.1285	0.3383968663	0.3471164384	5470	2.108773	9

myrcene r = 0.9, m-xylene,  $\alpha$ -pinene

C myrc (ug/m <sup>3</sup> )	C xyl (ug/m <sup>3</sup> )	Yield	Yield model
4.9424524632	12.2307304779	0.0030929191	0.0022125365
9.2029767653	22.7739425413	0.0586219909	0.048083519
7.4856013262	11.6141881266	0.0178663188	0.0163043305
16.1743232618	40.0254306843	0.1237089945	0.1111298341
20.0870438567	49.70795801	0.1980573917	0.1427753005
27.4781899445	67.9982939101	0.2305077086	0.196494925
41.2759589609	102.1426372884	0.2404441987	0.2337688354
48.0694549362	118.9540115798	0.2559946926	0.2518799315
58.6478414336	145.1315813396	0.2921892045	0.2798692031
75.3290706983	186.4114157322	0.2935121654	0.3013686191

myrcene  $r = 0.3$ , m-xylene,  $\alpha$ -pinene, isoprene

Start	Q1	Q4	Q2	Qiso	C myrc (ug/m3)	C xyl (ug/m3)	C pin (ug/m3)	C iso (ug/m3)	um3/cm3	Yield	Yield model	O3	std vol	datapoints
10:38	1.625	0.05	5.98	0.514	1.4105698702	10.4719064258	6.5656544309	218.4489077555	1.7592	0.0074260109	0.0063784145	5073	0.217317	13
12:01	1.625	0.071	5.98	0.514	1.9966020271	14.8225409023	9.2934063193	217.7501374489	3.8932	0.015964722	0.013293371	5122	0.168092	17
13:05	1.625	0.11	5.98	0.514	3.0750594046	22.8288828636	14.3132061949	216.4642114403	7.1282	0.027770618	0.0248276747	5049	0.299961	17
14:14	1.625	0.142	5.98	0.514	3.9504798998	29.3279026593	18.3879483081	215.4203816082	14.2179	0.0532332734	0.0432009062	5243	0.623791	18
15:04	1.625	0.204	5.98	0.514	5.6228035923	41.7430389749	26.171965033	213.4263440358	24.543	0.0855263623	0.0692360296	5114	0.523138	12
16:18	1.625	0.332	5.98	0.514	8.9792422637	66.6608487429	41.7948823376	209.4242092516	40.4494	0.1237517627	0.1093403606	5223	1.083866	12
16:59	1.625	0.532	5.98	0.514	10.2056802668	75.7657816327	47.5034745023	207.9618347908	53.3834	0.1563492995	0.1293675708	5331	1.117819	10
17:26	1.625	0.963	5.98	0.514	13.9788477961	103.7773379051	65.0661036502	203.4628027828	71.4399	0.1849408679	0.1649618062	5283	1.258599	7
17:50	1.625	0.8	5.98	0.514	17.1021377672	126.9642788773	79.6038033843	199.7386687651	88.2394	0.2085440394	0.1918687197	5276	1.602461	6
					20.248465546	150.3222498502	94.2487361577	195.9870650331	107.3926	0.2330535618	0.2170413677	5225	2.303578	7

myrcene  $r = 0.9$ , m-xylene,  $\alpha$ -pinene, isoprene

C myrc (ug/m3)	C xyl (ug/m3)	C pin (ug/m3)	C iso (ug/m3)	Vol (um3/cm3)	Yield	Yield model
1.4105698702	10.4719064258	6.5656544309	218.4489077555	0.0074260109	0.0074260109	0.0058763629
1.9966020271	14.8225409023	9.2934063193	217.7501374489	0.015964722	0.015964722	0.0121530311
3.0750594046	22.8288828636	14.3132061949	216.4642114403	0.027770618	0.027770618	0.0224299814
3.9504798998	29.3279026593	18.3879483081	215.4203816082	0.0532332734	0.0532332734	0.0389100354
5.6228035923	41.7430389749	26.171965033	213.4263440358	0.0855263623	0.0855263623	0.0620050808
8.9792422637	66.6608487429	41.7948823376	209.4242092516	0.1237517627	0.1237517627	0.0973142665
10.2056802668	75.7657816327	47.5034745023	207.9618347908	0.1563492995	0.1563492995	0.1152678091
13.9788477961	103.7773379051	65.0661026502	203.4628027828	0.1849408679	0.1849408679	0.1467567183
17.1021377672	126.9642788773	79.6038033843	199.7386687651	0.2085440394	0.2085440394	0.1707469562
20.248465546	150.3222498502	94.2487361577	195.9870650331	0.2330535618	0.2330535618	0.19333536796

toluene

Start	Q1 (l/min)	Q4 (l/min)	Q2 (l/min)	C (ug/m3)	Vol (um3/cm3)	Yield	Yield model	O3 (ppb)	std vol	datapoints
10:56	1.45	0.2	6.06	6.06	38.0545	0.1440459736	0.1341052	4915	0.60621	21
12:00	1.45	0.106	6.06	6.06	142.1515433958	9.8706	0.0694371638	5093	0.227672	11
12:39	1.45	0.049	6.06	6.06	66.3246839836	1.0441	0.0157422537	5184	0.216658	10
13:43	1.45	0.07	6.06	6.06	94.424957925	3.8173	0.0404268118	5194	0.080925	11
14:19	1.45	0.153	6.06	6.06	203.6288514595	20.2724	0.0995556369	5229	0.328972	14
14:53	1.45	0.301	6.06	6.06	391.2824187934	57.2718	0.1463694693	5359	0.969958	11
15:23	1.45	0.399	6.06	6.06	510.8070064804	83.6412	0.1637432512	5043	1.348106	10
15:59	1.45	0.601	6.06	6.06	746.0780668715	134.1336	0.1797849393	5265	2.139729	8

toluene,  $\alpha$ -pinene

Start	Q1 (l/min)	Q4 (l/min)	Q2 (l/min)	CQ7a tol (ug/m <sup>3</sup> )	CQ7a pin (ug/m <sup>3</sup> )	Vol (um <sup>3</sup> /cm <sup>3</sup> )	Yield	Yield model	O3 (ppb)	std vol	datapoints
11:01	1.455	0.028	6.1	37.6524740705	4.3851146629	0.22542	0.0059623437	0.005657146	5475	0.050266	11
11:36	1.455	0.052	6.1	69.653229945	8.1120140839	2.5279	0.0325068098	0.0338574569	5059	0.062134	13
12:13	1.455	0.072	6.1	96.1304161623	11.1956228076	6.3847	0.0650792673	0.0659573255	5069	0.147781	20
13:14	1.455	0.095	6.1	126.367832958	14.7171387235	14.0396	0.0995116478	0.0993303808	5100	0.32949	16
13:59	1.455	0.165	6.1	217.0286716576	25.2757789191	31.0579	0.1281771751	0.1436763576	5251	0.383875	15
14:37	1.455	0.237	6.1	308.190240885	35.8927156622	60.7198	0.1764684907	0.1780685644	5282	0.697213	19
15:26	1.455	0.431	6.1	543.8158105074	63.3343423895	112.7475	0.1856995332	0.20228838412	5294	1.347151	7
15:53	1.455	0.601	6.1	739.0759962456	86.0749012692	167.6029	0.2031178788	0.21356636956	5307	3.298838	10